POST-PALEOGENE DEFORMATION IN NORTHERNMOST TIP OF TUZGÖLÜ FAULT ZONE (PAŞADAĞ, SOUTH OF ANKARA), TURKEY

A THESIS SUBMITTED TO
THE GRADUATE SCHOOL OF NATURAL AND APPLIED SCIENCES
OF
MIDDLE EAST TECHNICAL UNIVERSITY

BY

G. DİLARA ÇELİKER

IN PARTIAL FULFILLMENT OF THE REQUIREMENTS
FOR
THE DEGREE OF MASTER OF SCIENCE
IN
GEOLOGICAL ENGINEERING

DECEMBER 2009

POST-PALEOGENE DEFORMATION IN NORTHERNMOST TIP OF TUZGÖLÜ FAULT ZONE (PAŞADAĞ, SOUTH OF ANKARA), TURKEY

submitted by **G. DİLARA ÇELİKER** in partial fulfillment of the requirements for the degree of **Master of Science in Geological Engineering Department, Middle East Technical University** by,

Prof. Dr. Canan ÖZGEN ____________________
Dean, Graduate School of **Natural and Applied Sciences**

Prof. Dr. M. Zeki ÇAMUR ____________________
Head of Department, **Geological Engineering**

Assoc. Prof. Dr. Bora ROJAY ____________________
Supervisor, **Geological Engineering Dept., METU**

Examining Committee Members:

Prof. Dr. Kadir DİRİK ____________________
Geological Engineering Dept., HÜ

Assoc. Prof. Dr. Bora ROJAY ____________________
Geological Engineering Dept., METU

Prof. Dr. Vedat TOPRAK ____________________
Geological Engineering Dept., METU

Prof. Dr. Erdin BOZKURT ____________________
Geological Engineering Dept., METU

Assoc. Prof. Dr. M. Lütfü SÜZEN ____________________
Geological Engineering Dept., METU

Date: 01.12.2009

I hereby declare that all information in this document has been obtained and presented in accordance with academic rules and ethical conduct. I also declare that, as required by these rules and conduct, I have fully cited and referenced all material and results that are not original to this work.

Name, Last name: G. Dilara Çeliker

Signature :

ABSTRACT

POST-PALEOGENE DEFORMATION
IN NORTHERNMOST TIP OF TUZGOLU FAULT
(PAŞADAĞ, SOUTH OF ANKARA),
TURKEY

Çeliker, G. Dilara
M.Sc., Department of Geological Engineering
Supervisor: Assoc. Prof. Dr. Bora Rojay

December 2009, 73 pages

The research area is located to the northern tip of Tuzgolu fault zone in the junction of neotectonic structures, namely, Eskişehir-Cihanbeyli, Sungurlu-Kırıkkale and Tuzgölü fault zones (Central Anatolia).

The study is carried out in Paleocene sequences of Paşadağ group on the structural analysis of bed, gash vein, fault and fault plane slippage data. The method of study based on i) the rose and stereo analysis of the planar structure (beds, gash veins and faults) on ROCKWORKS 2009 software and ii) on fault slip analysis on ANGELIER 1979 software.

The bed analyses done on 605 measurements manifest N10°-20°E bedding attitude. The analysis done on 64 gash veins shows a general trend of NNE-SSW (N15°E). The final analysis done on 160 fault planes pointed out a general trend of NNW-SSE (N20°W).

Analysis based on the fault plane slip data manifest two stages of faulting under almost NE-SW compression during post-Paleocene – pre-Miocene period and one stage of faulting under WNW-ESE extension most probably during post-Miocene.

To conclude, the Paleocene sequences are deformed continuously under WNW-ESE directed compression which is followed by a NE-SW to N-S compression resulted in the development of a reverse to dextral strike slip faulting during post-Paleocene – pre-Miocene period.

Keywords: gash vein, dextral strike slip faulting, Paleocene, Tuzgölü Fault Zone.

ÖZ

TUZGÖLÜ FAYININ KUZEY UCUNDAKİ
PALEOSEN SONRASI DEFORMASYONU
(PAŞADAĞ, GÜNEY ANKARA),
TÜRKİYE

Çeliker, G. Dilara
Y.Lisans, Jeoloji Mühendisliği Bölümü
Tez Yöneticisi: Doç. Dr. Bora Rojay

Aralık 2009, 73 sayfa

Çalışma alanı Orta Anadolu'da Tuz Gölü fay zonunun kuzey ucunda Eskişehir-Cihanbeyli, Sungurlu-Kırıkkale ve Tuzgölü fay zonlarının, kesişme noktasında yer alır.

Çalışma, Paleojen yaşlı Paşadağ grubu üyesi Paleosen serisinde tabaka, açılma çatlağı damarı, fay düzlemi ve fay düzlemi kayma verileri üzerinden yapılmıştır. Çalışma metodu, i) düzlemsel yapıların ROCKWORKS 2009 yazılımı vasıtası ile gül ve stero analizlerinin, ve ii) ANGELIER 1979 yazılımı vasıtası ile de fay düzlemi kayma analizlerinin çalışılmasına dayanır.

605 adet tabaka ölçümü üzerinde yapılan tabaka analizinde, tabaka yönelimi K10°-20°D bulunmuştur. 64 açılma çatlağı damarı üzerinde yapılan analiz neticesinde genel yönelim KKD-GGB (K15°D) olarak bulunmuştur. 160 fay üzerinde yapılan son analizde genel yönelim KKB-GGE (K20°B) olarak bulunmuştur.

Fay düzlemi atım verilerine dayanan analizler neticesinde, Paleosen sonrası – Miyosen öncesi dönemde gelişmiş KD-GB sıkışmalı iki fazlı faylanma ve muhtemelen Miyosen sonrası dönemde de BKB-DGD yönelimli bir genişleme rejimi bulunmuştur.

Özet olarak, Paleosen serisi, Paleosen sonrası – Miyosen öncesi dönemde BKB-DGD yönlü sıkışmayı takip eden KD-GB dan K-G ye değişen sıkışma rejimi altında ters faylanmadan sağ atımlı yanal faylanmaya değişen sürekli bir sıkışma etkisinde deforme olmuştur.

Anahtar kelimeler: Açılma çatlağı damarı, Sağ yanal atımlı faylanma, Paleosen, Tuz Gölü Fay Zonu.

To My Parents

ACKNOWLEDGMENTS

First of all, I would like to express my gratitude to my supervisor Assoc. Prof. Dr. Bora Rojay for his clear guidance, valuable criticism and continuous support during every stage of this thesis. Without any hesitation, he shared his vast geological knowledge with me generously. His friendly and humorous manner towards me always encouraged me to complete this study.

Secondly I would like to express my highest gratitude to my family. Every member in my family showed extreme patience and gave unlimited encouragement during this study.

Then, I would like to thank to Şule Deveci Gürboğa (MSc.) for her technical support on structural geology.

Lastly, I would like to thank to my examining committee members; Prof. Dr. Vedat Toprak, Prof. Dr. Kadir Dirik, Prof. Dr. Erdin Bozkurt and Assoc. Dr. M. Lütfi Süzen for their support and guidance.

TABLE OF CONTENTS

LIST OF FIGURES

CHAPTER 1

INTRODUCTION

1.1. Purpose and Scope

The paleotectonic structures are very important geological structures in the identification of paleotectonic deformational settings and neotectonic structures.

There are two main aspects in choosing a research area in the northern tip of the "Tuzgölü" fault zone, as: 1) paleostructures – pre-Miocene – Pliocene structures- should be well documented and defined, such as, Tuzgölü Fault Zones in order to understand the seismotectonics of the region where junction of faults displays a complex deformational resolutions when linked with the seismic events. The seismic records –the focal mechanism solutions- and the faults on surface between Paşadağ and Bala (Figure 1) displays contradictory results. There are two issues that should be clarified. Firstly, the structures should be clearly identified whether they are resurrected or replaced or totally new structures (Şengör et al 1985). Secondly, the structures should be classified as being paleotectonic or neotectonic structures. A neotectonic period is defined as the time that elapsed since the last major wholesale tectonic reorganization in a region of interest, and the structures evolved during this period are classified as neotectonic structures (Şengör, 1980; Şengör et al 1985). So the collision of Arabian plate with Anatolia in Middle to Latest Miocene, which is accepted as the last major tectonic event in the evolutionary history of Turkey, is drastic enough forming a land-mark to separate the country's neotectonic development from its paleotectonic development. Therefore paleotectonic structures should be well identified to be able to fit the neotectonic frame of the Anatolia correctly.

And, secondly, 2) the pre-Neotectonic period structures –Paleotectonic structures- are still not well defined in the Tuzgölü to Haymana to Ankara region which may help to configure the paleotectonic settings with plate tectonic kinematics. The existence of poor and scarce deformational analysis done in the region is another reason to choose this sector in central Anatolia.

To fulfill the above issues, the northern tip of the "Tuzgölü" Fault zone to the north of Paşadağ Mountain is chosen as a research area where Paleogene (Paleocene-Eocene) stratigraphy is well-established; pre-Miocene-Pliocene unconformity is clearly pronounced.

The thesis aims to analyze the deformational structures developed during post-Paleocene – pre-Latest Miocene period in the northern tip of Tuzgölü fault zone (northern limb of the Paşadağ Mountain). For this purpose, i) structural data (strike/dip measurements of the beds and faults), and ii) slip-lineation data from the fault planes were collected and analyzed for structural purposes.

1.2. Study area

The research area is located within an economically important region where economical salt deposits were situated, namely, Keskin-Kırşehir rock-salt deposits, Şereflikoçhisar salt lake deposits and Tuzgölü salt dome far to the south that is planning for natural gas storage in Turkey.

The research area is situated in Central Anatolian "Ova" Province (Şengör et al 1985) between the North Anatolian Ophiolitic Accretionary wedge to the north, Tuzgölü Basin to the south and Kırşehir Crystalline Complex to the east (Figure 1). On the other hand, it is just in the junction of faults, namely, southwestern tip of the NE-SW trending "Sungurlu-Kırıkkale" fault, northern tip of the NNW-SSE trending "Tuzgölü" fault and southeastern tip of the NW-SE trending "Dereköy fault" (Figure 1). Quite linear, N50°W trending Tuzgölü Fault Zone extends between Bor districts in the southeast, Paşadağ Mountain in the north where the research area is situated to the northeast of the zone (Figure 1).

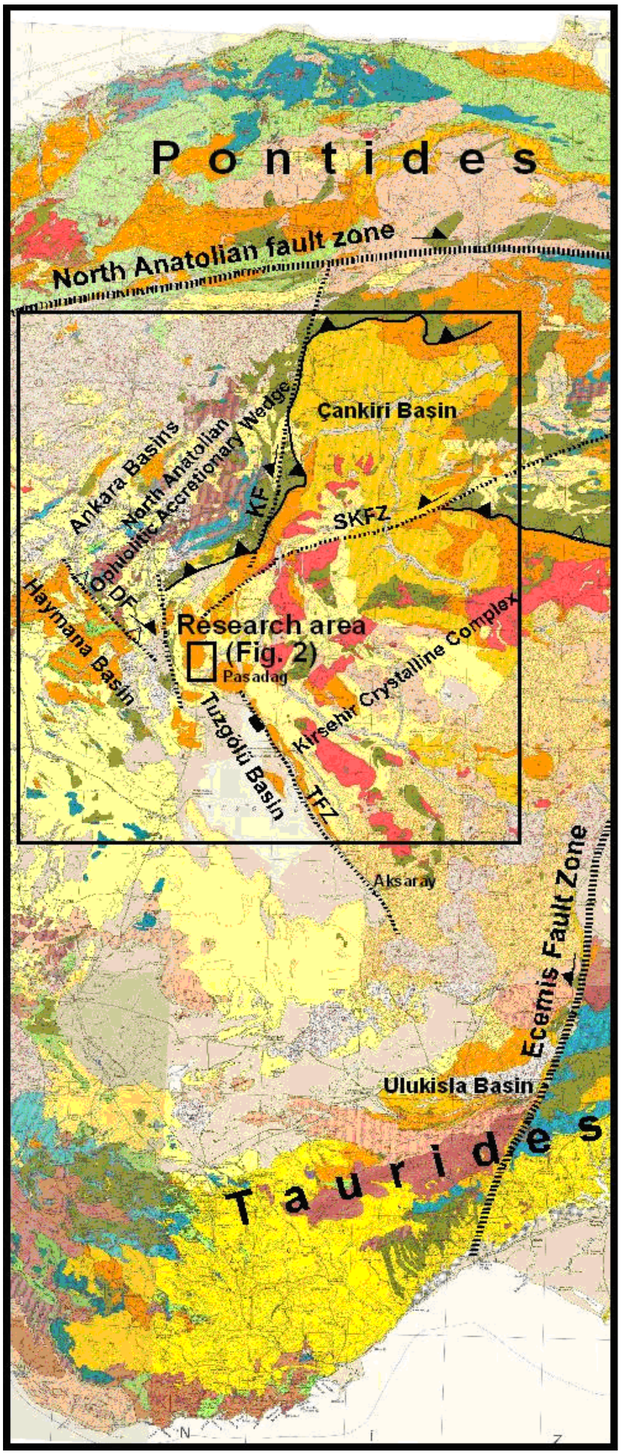

Figure 1. Some of the interpreted major structures of Central Anatolia, from the Pondides in the north and Taurides in the south (interpreted on 1:500 000 geological map of the MTA). DF. Dereköy Fault, KF. Kalecik Fault, SKFZ. Sungurlu-Kırıkkale Fault, TFZ. Tuzgölü Fault Zone.

1.3. Methods of Study

The thesis involves a series of geological surveys as preliminary office studies, field surveys and final office studies on structural analysis.

Preliminary office studies are the literatures surveys about the geology of the region and aerial photographic surveys carried out on 1: 60 000 scale. Later, extensive field studies were conducted in the areas spotted by aerial photographic surveys and 1:25000 scale geological map of the area with the geological structures were prepared (Figure 2). Attitude of beds, en echelon veins and types of the faults were determined by using fault plane markings like slickenlines and “fault steps” (chatter marks). Numerous dip and strike measurements of beds, en echelon veins and striae data from the faults were collected over the study area for structural analysis.
Bidirectional rose diagrams of the strike data at 10^0 class intervals were created by Rockworks 2002 software for the analysis of bedding planes and en echelon veins. The same program was also used for creating contoured stereonet diagrams of the bedding data for the fold analysis. For this purpose, Schmidt net (equal-area net), which is commonly preferred in structural analyses to prevent preferred alignment of the data, was used.

For the analysis of the slip data, although the software analyzing the fault slip data having alike algorithms, the software Tensor v.5.42 (Angelier Inversion Method) was used. Different deformational phases with principal paleo-stress directions of those deformational stages were calculated by using that software and by field observations.

And finally, all structural data analysis used to interpret the stresses acting in the region since post-Paleogene to pre-Neogene is kinematically analyzed. Unfortunately during the structural analysis no joint survey analysis is done.

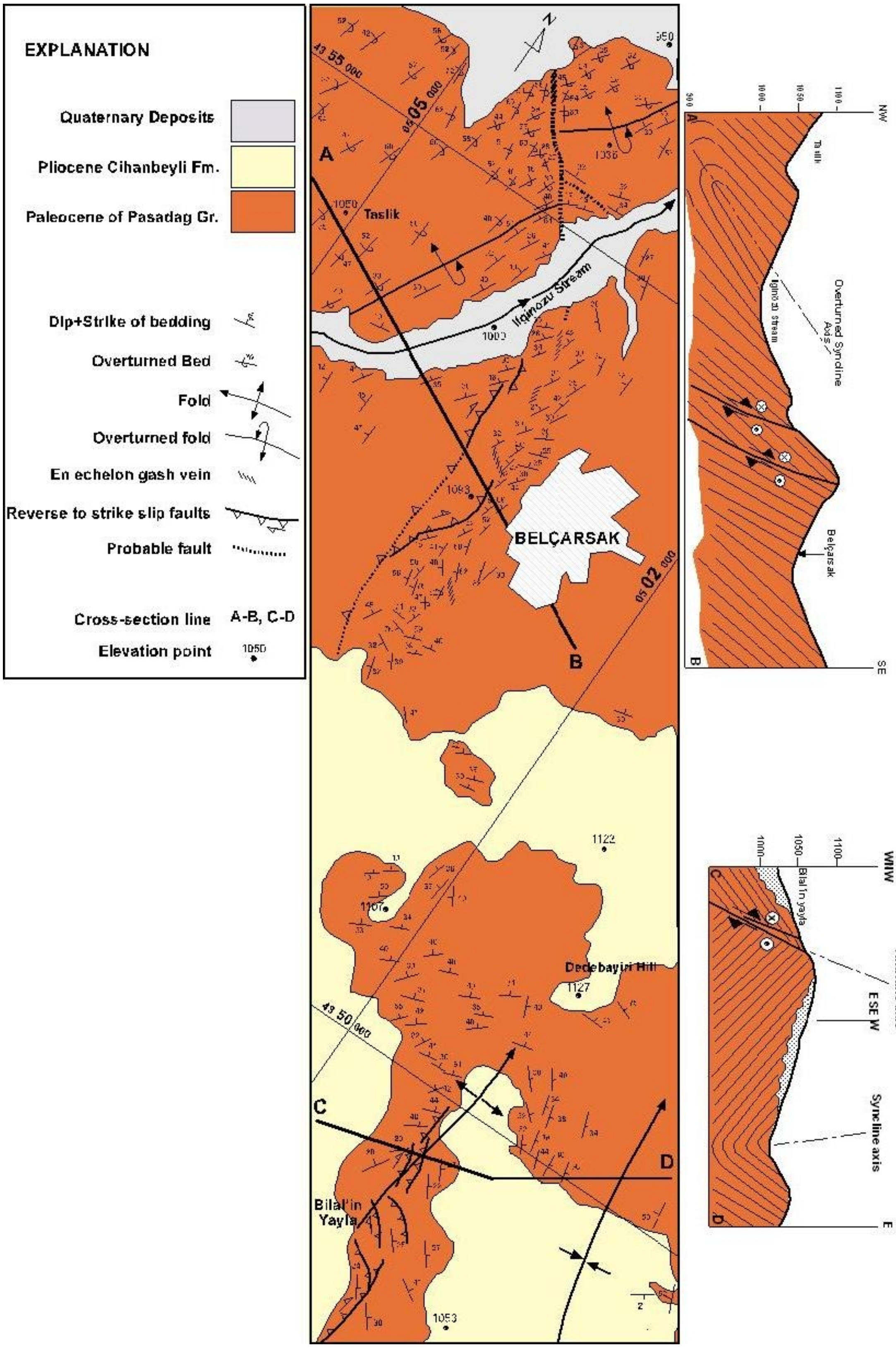

Figure 2. Geological map of the NW of Paşadağ region with geological cross sections.

CHAPTER 2

REGIONAL GEOLOGY

2.1. Tectonic Setting

Turkey, which is located just on the tremendous Alpine-Himalayan orogenic belt, has quite complicated regional geology. Its tectonic structure is composed of several amalgamated pre-Alpine and Alpine microcontinents of different origin and characteristics. Complex geological history of Turkey involves interactions of those microcontinents, and opening and closure of the oceans separating them at different geological times. The mentioned oceanic basins are collectively known as Tethys Ocean. It is a triangular shaped, gigantic embayment, which narrows down from east to west, and separates Laurasia and Gondwana continents of Permo-Triassic Pangea (Şengör and Yılmaz, 1981).

The entire Anatolia that is shaped during post-Miocene when the N-S compression evolved in between North Anatolian, East Anatolian Fault Zones and Mediterranean Subduction Zone. The study area lies between the North Anatolian Fault Zone in north, Kırşehir crystalline complex in east, Aegean horst and graben in the west and Tuzgölü Basin to the south within the Central Anatolia, to the northern tip of the Tuzgölü fault zone.

Numerous authors studied the geology of Turkey, defined the tectonic units of Turkey and evaluated the tectonic evolution by using various global tectonic models (Lahn, 1949; Ketin, 1966; 1983; Brinkmann, 1976; İlhan, 1976; Şengör and Yılmaz, 1982). Recently, Anatolia is genetically differentiated into various tectonic terrains (Göncüoğlu et al 1997).

2.2. Previous Studies on Geology

Basically the studies are concentrated on the i) stratigraphy-tectonostratigraphy and ii) neotectonics of the central Anatolia. The stratigraphic studies are mainly done for oil exploration surveys. Oil shows in the region led surveys to concentrate in thick Upper Cretaceous to Paleogene sequences in the Central Anatolian basins extending from Ankara to Haymana to Tuzgölü and to Çankırı.

Most of the Paleogene stratigraphy displays a correlative stratigraphy except the Paleocene sequences in the basins on top of the Cretaceous accretionary wedge of “Ankara mélange” belt like the Alçı and Orhaniye Basins (Koçyiğit and Lünel 1987; Koçyiğit et al 1988; Gökten et al 1988). On the other hand, the Paleocene sequences are correlative sequences in Kırıkkale (Norman 1972), Çankırı (Akyürek et al 1984; Dellaoğlu et al 1992; Kaymakçı, 2000), Haymana (Lokman and Lahn 1946; Yüksel 1970; Ünalan et al 1976; Çiner 1993; Görür and Derman 1978) and Tuzgölü (Arıkan 1975; Turgut 1978; Derman 1980; Uygun 1981; Dellaoğlu and Aksu, 1984; Görür et al 1984; Oktay and Dellaloğlu 1991; Göncüoğlu et al 1992) Basins with Paşadağ Mountain sequence where the research area lies (Figure 1). Almost all of the researchers linked the Upper Cretaceous to Paleogene sequence evolutions to the existence of the accretionary wedge paleo-high developed during the northward subduction of the Neotehys (Görür et al 1998).

Second group of studies are concentrated on the neotectonic evolution of the central Anatolia and the role of the Tuzgölü Fault zone and the fault zone extending from İnonu-Eskisehir to Cihanbeyli-Kulu fault zone (Erol, 1961; 1993; Koçyiğit 1991; 1992; 2000; Koçyiğit et al 1995; Toprak and Göncüoğlu 1993; Dirik and Göncüoğlu 1996; Çemen et al 1999; Dirik and Erol, 2000). The faults have a junction point in the research area which causes conflicts in the neotectonic interpretation of the region.

Within this frame, the paleotectonic setting of the Tuzgölü fault zone is the main concern of this thesis, where the Şereflikoçhisar-Aksaray Fault Zone terminology is used in literature (Derman et al 2000). However, “Tuzgölü Fault Zone” term is preferred in this study.

There are scarce previous tectonic studies done on the structural analysis of the paleotectonic setting in the region. Since pioneer studies on the tectonic evolution of central Anatolia (Chaput 1936; Egeran and Lahn, 1951; Bailey and McCallien 1950), the studies are concentrated on the stratigraphy and related paleotectonic settings of the stratigraphic sequences. None of these studies support the paleotectonic evolutions with structural data except Şahbaz and Köksoy 1985 and Derman et al 2000 where both focused on the attitude of folding developed in Paleocene sequences. The NE-SW trending folding is analyzed and mapped in Paşadağ region (Şahbaz and Köksoy 1985). Paleotectonically the terrain is interpreted as a huge s-shape structure –Ankara virgation- from Haymana to Kırıkkale (Şahbaz and Köksoy, 1985). The Eocene, Oligo-Miocene and Pliocene deformational periods affected the region where compression continues until the end of Pliocene (Şahbaz and Köksoy 1985). In Derman et al 2000, a sinistral strike slip motion is proposed for the evolution of the so called “Tuzgölü Fault” by analyzing the en echelon faulting of pre-Middle Eocene in age, which was named as Şereflikoçhisar-Aksaray Fault Zone (Derman et al 2000).

2.3. Tectonic Evolution of Turkey

The main tectonic events in the complex geological history of Turkey during Paleozoic to Mesozoic times can be summarized as the simultaneous evolution of Tethys Ocean. The southward subduction of the Paleotethyan oceanic crust is believed to initiate back-arc spreading in the northern margin of Gondwana (Şengör and Yılmaz, 1981). This spreading event gave way to the formation of oceanic basin (Mesozoic Tethys), named as Neotethys. It continued to evolve during Middle Mesozoic after the total consumption of Paleotethys under Gondwana. There were two main branches of Neotethys; northern Neotethys (also known as İzmir-Ankara ocean or Vardar ocean), which is surrounded by Sakarya Continent at north and Tauride-Anatolide Platform at south, and southern Neotethys at the south of Tauride-Anatolide Platform. The northward subduction in northern Neotethys

Ocean during Cretaceous gave rise to the total consumption of the oceanic crust and collision of Sakarya Continent with Tauride-Anatolide Platform took place diachronously from Late Mesozoic to Early Paleogene in central Anatolia (Şengör and Yılmaz, 1981). After the collision, continental to shallow marine deposition in fault controlled basins was predominated in the region (Şengör and Yılmaz, 1981). While the ophiolites and mélange of the closed İzmir-Ankara ocean were being obducted on the Tauride-Anatolide Platform, which was also being internally deformed due to the compressional tectonics, the southern Neotethys remained open. This distinctive collision event marks the beginning of a new tectonic era, neotectonic period in the area where proto-Anatolia was located (post - Middle Miocene: Şengör 1980; post-Early Pliocene: Koçyiğit, 1992). A tectonic escape model in which the Anatolian block escapes westward along the major strike-slip faults, North Anatolian and East Anatolian Fault Zones due to the post-collision convergence of Arabian platform and Eurasia is the time of initiation of the neotectonic period. Further westerly motion of Anatolian block is obstructed at eastern Mediterranean which results in an N-S extensional regime in the western Turkey (Şengör et al 1985).

Before the total closure of İzmir-Ankara ocean and related oceans, Paleocene paleogeographical setting around Ankara is represented by shallow to deep marine environment that are mainly characterized by reefal, platform limestones and flyschoidal sediments extending from Polatlı-Haymana-Tuzgölü to Kırıkkale-Sungurlu-Çankırı depositing on top of the accreted North Anatolian Ophiolitic masses. Terrestrial sequences consisting mainly of fluvial and lacustrine environments in Paleocene age occur along a NE-SW trending belt covering northwest of Ankara extending towards Nallıhan-Göynük where marine sequences ocean are present. Paleocene volcanics and volcaniclastics rocks, with numerous volcanic centers which are interpreted as members of a magmatic-arc formed by northward subduction of İzmir-Ankara Ocean, occur along this belt. Interbedded sequences of volcanics, volcaniclastics and terrestrial sediments imply that the paleogeographic setting is composed of a continental deposition with small lakes around the terrestrial volcanic vents. After the entire consumption of the northern

Neotethys and consequent collision during post-Paleocene-Eocene period, paleogeography of the Ankara and its vicinity has changed considerably. The land area of central Anatolia including Ankara was uplifted due to collision and formed highlands relative to its surroundings where lake settings evolved with volcanism during Miocene. After the Late Miocene, the present tectonic regime of Turkey was established and operating till present. Turkey acquired its today's geography, and as a result of its complicated geological history, it is a complex mixture of different amalgamated microcontinents, remnants of consumed oceans (ophiolites, mélanges) in the form of linear belts, magmatic arcs produced by subduction zones, crustal massifs (e.g. Menderes Massif, Kırşehir Massif) and finally a vast collection of tectonically controlled Tertiary basins filled by shallow marine to molassic to fluvial to lacustrine deposits mostly interbedded with volcanics/volcaniclastics. Later continental deposition in fluvial to lacustrine environments became predominant in the central Anatolia during Plio-Quaternary.

CHAPTER 3

STRATIGRAPHY

The stratigraphy of the region constructed on the Paleocene Kırşehir crystalline massif and Cretaceous Ankara Mélange at the base of Upper Cretaceous-Paleocene-Eocene sedimentary sequence (Paşadağ Group). The Paleogene units are unconformably overlain by Neogene units interbedded with volcanics (Oligo-Miocene gypsum masses with gypsum bearing sequences (Mezgit formation) and Miocene-Pliocene continental clastics (Cihanbeyli Formation) (Figure 3).

3.1. Paşadağ Group (Tp)

The sequence which is characterized by a quite thick sedimentary sequence is mainly composed of shale, sandstone and conglomerate alternation (Figure 4). The sequence is very much similar to Paleocene sequences of Haymana (Ünalan et al 1976) and Tuzgölü (Göncüoğlu et al 1992) basins. Although the unit is composed of many formations, at this stage, it is kept under Paşadağ group heading for unifying purposes (Şahbaz and Köksoy 1985).

The sequence is gradual continuation of the Upper Cretaceous sequence (Arıkan 1975; Turgut 1978; Uygun 1981; Derman 1980; Dellaloğlu and Aksu 1984; Görür and Derman 1984; Göncüoğlu et al 1992: Derman et al 2000). It unconformably overlies Cretaceous Ophiolitic Mélange and is unconformably overlain by the Oligo-Miocene sedimentary sequence with huge gypsum masses (Mezgit Formation) (Şahbaz and Köksoy 1985).

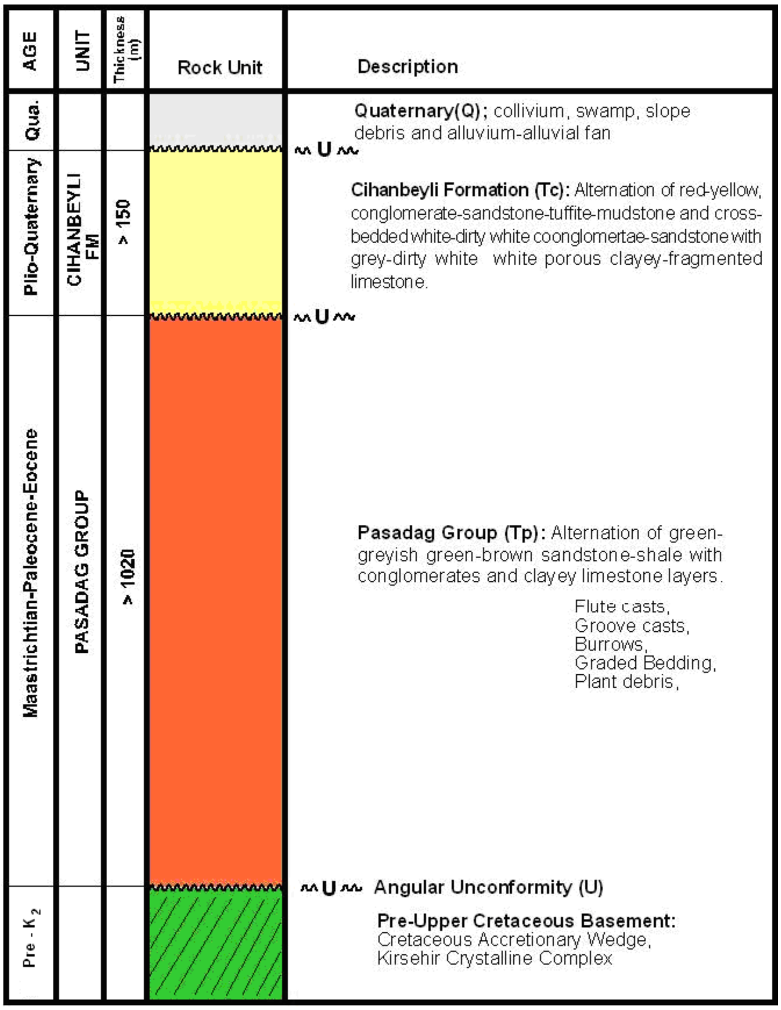

Figure 3. Stratigraphic columnar section of the research area.

It is hard to measure the thickness of the sequence in the study area due to the extensive folding and overturning of beds (Figure 2, 4). But it is above 1020 m when correlated with sedimentary sequences of Paleocene age in Haymana, Kırıkkale and Tuzgölü regions.

Due to its thick and regional distribution, the sequence is represented by different rock types (Şahbaz and Köksoy, 1985). But, in the study area, general and dominant rock group is dark green-gray colored shales; brown colored sandstone, gray biodetrital clayey limestone and gray-brown colored conglomerate alternation.

Green-gray colored shales are thin bedded and highly jointed, easily separated and friable (Figure 5). Medium to thick bedded, frequently jointed brown colored sandstones are alternated with shales (Figure 6). Flute casts, groove and load casts, borrowings and bounce marks and zones of plant debris observed at the bottom of beds (Figure 7, 8, 9, 10). In some areas, en echelon veins as gash veins are cropped out. Dark gray, locally yellowish brown colored conglomerates are massive-thick bedded, place to place graded bedded and less jointed (Figure 11). The gray colored biodetrital clayey limestones are rich in fossil fragments. Debris flows and slump structures are also exist in the sequence.

The age of the sequence is Danian to Thanetian (Paleocene) where the top levels which are Lutetian (Eocene) are missing in the study area. The Lutetian section is characterized by the existence of Paleocene limestone olistoliths in shale-sandstone alternating sequence which is cropped out in Haymana and Tuzgölü basins.

The depositional setting for the Paleocene units is slope to basin pelagic environment (Şahbaz and Köksoy, 1985).

Figure 4. General view of folded Paleocene sequence of the Paşadağ Group. Locality: Taşlık locality, Facing northeast.

Figure 5. Alternation of highly jointed sandstones and friable shales. Marker points the dip direction. Locality: Taşlık locality.

Figure 6. Alternation of the shales and sandstones. Locality: Taşlık locality.

Figure 7. Flute casts on dip face of the overturned beds. Marker points the dip direction.

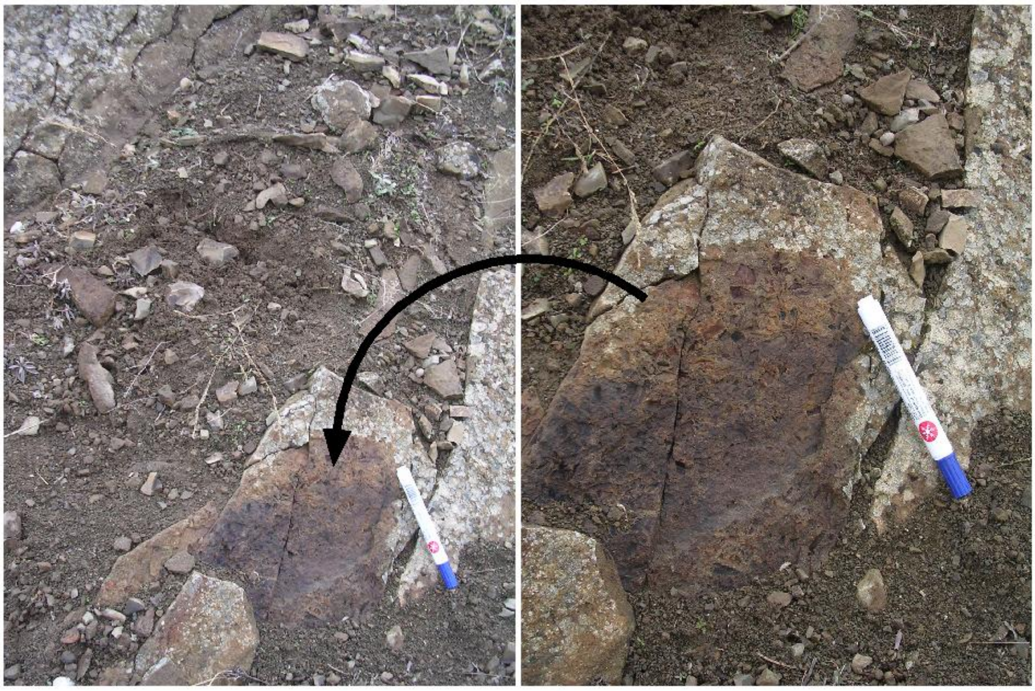

Figure 8. Plant debris accumulation on the bottom of the overturned beds. Marker points the dip direction.

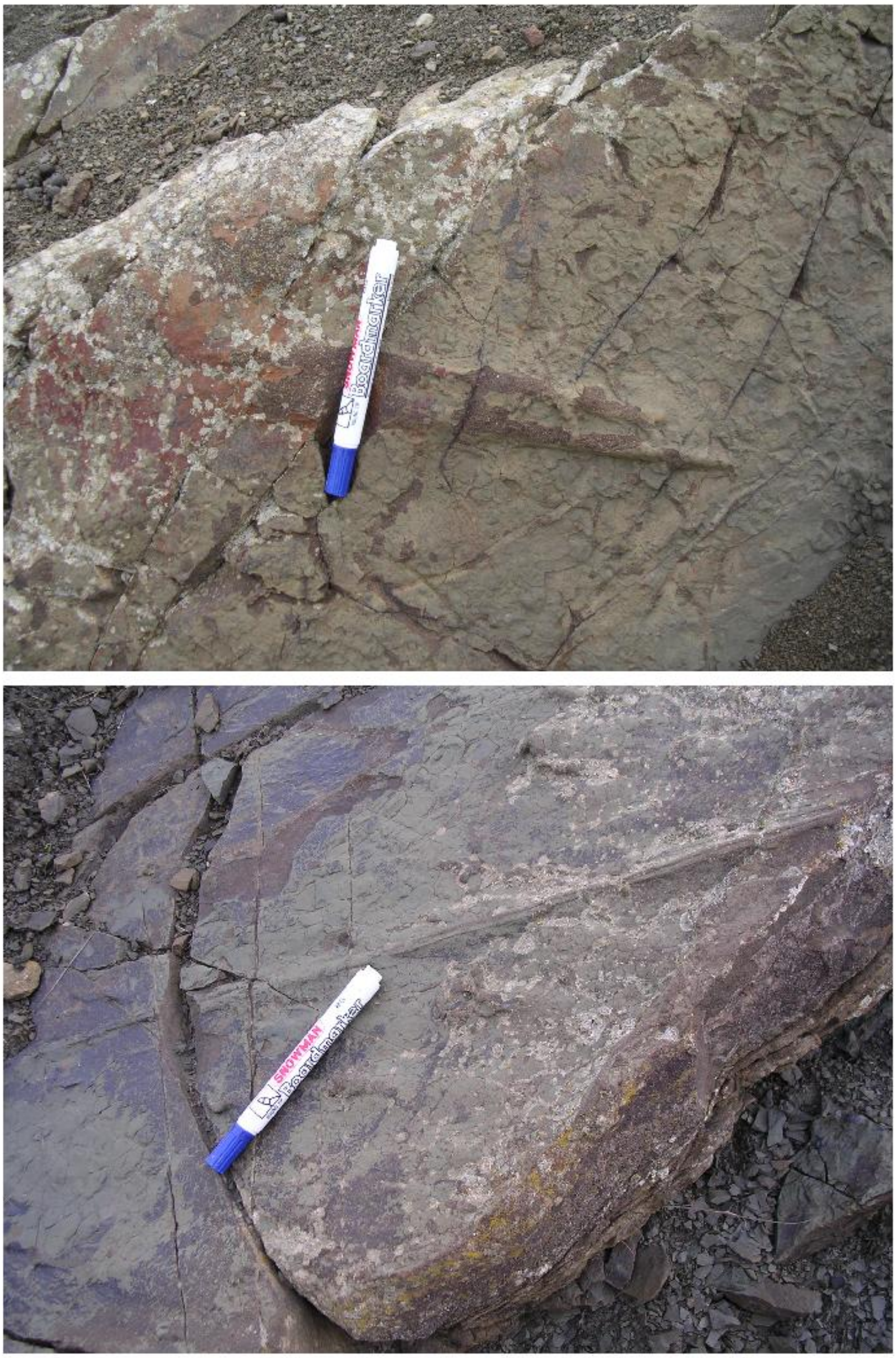

Figure 9. Groove casts on dip face of the overturned beds. Marker points the dip direction.

Figure 10. Burrows on dip face of the overturned beds. Marker points the dip direction.

Figure 11. Overturned graded bedding (coarsening upward). Marker points the dip direction, candy is on the bottom of the overturned bed.

3.2. Cihanbeyli Formation (Tc)

The unit is generally composed of red colored conglomerate-pebbly mudstone-sandstone alternation, yellow colored conglomerate, sandstone and green colored tuffite-mudstone alternation and on the topmost, in high topographies, it is ended with white-dirty white, cross-bedded conglomerates-sandstones and grey-dirty white, porous, pebbly clayey limestones. In gravelly mudstone-sandstone alternation, conglomerate lenses are widely cropped out. Tuff bands are seen in southernmost extension (Peçenek valley) (Göncüoğlu et al 1992). The thickness of the unit exceeds 150m.

The bedding is very distinctive and mostly almost horizontal. Although it is rare, the bedding gets steeper in zones affected by faults. In regional scale open folding exists.

Depositional environment of the unit is interference of terrestrial river deposits and lacustrine units where volcanism effective. The unit can be correlative with the Gölbaşı formation (Akyürek et al 1984), Pecenek formation and Kızılırmak formation (Göncüoğlu et al 1992) in central Anatolia.

3.3. Quaternary units (Qal)

Quaternary units may differentiate into three main groups, but mapped as single unit. They are colluviums, terrace gravel, slope debris, alluvial fan, alluvium, and swamp deposits.

CHAPTER 4

STRUCTURAL GEOLOGY

Description of the observed geological structures together with the analysis and interpretation of the structural data gathered during the extensive field studies will constitute the main subject of this chapter. Principally three types of structural data were collected from Paleocene section of the Paşadağ Group : (i) dip-strike measurements of bedding planes (Figure 4, 5), (ii) dip-strike of en echelon gash veins (Figure 12) and (iii) dip-strike and slip-lineation data from the fault planes (Figure 13, 14, 15).

The structural data was gathered from a belt extending in NW-SE trend around Belçarşak village (NW of Paşadağ Mountain) (Figure 2). A fault extends in NNW-SSE trend for 4 kilometers with a narrow zone –maximum 370 meters- and steps in SE direction and continuous in NNW-SSE trend for 2 kilometers in a 11o meters width (Figure 2). Overall, the fault displays a SE stepping pattern.

An overturned structure with various scales of folds is cropped out in the study area where the mega scale ones are mapped (Figure 2). The meter scale folds which can not mapped are mainly observed in the areas where there is faulting of various scales.

Finally, gash veins are gathered from the North and West of the Belçarşak village (Figure 2). The veins are not continuous for long distances and do not cropped out in the South of the Belçarşak village.

Figure 12. Gash veins. A, B: en echelon gash veins, C: equant granular calcite crystal growth at extensional bends along veins, D: perpendicular to angular crystal fibers at acute angle to vein walls

Figure 13. General view of the N15°W/51°S trending reverse to dextral strike slip fault. Locality: east of the “Bilal’in yayla.

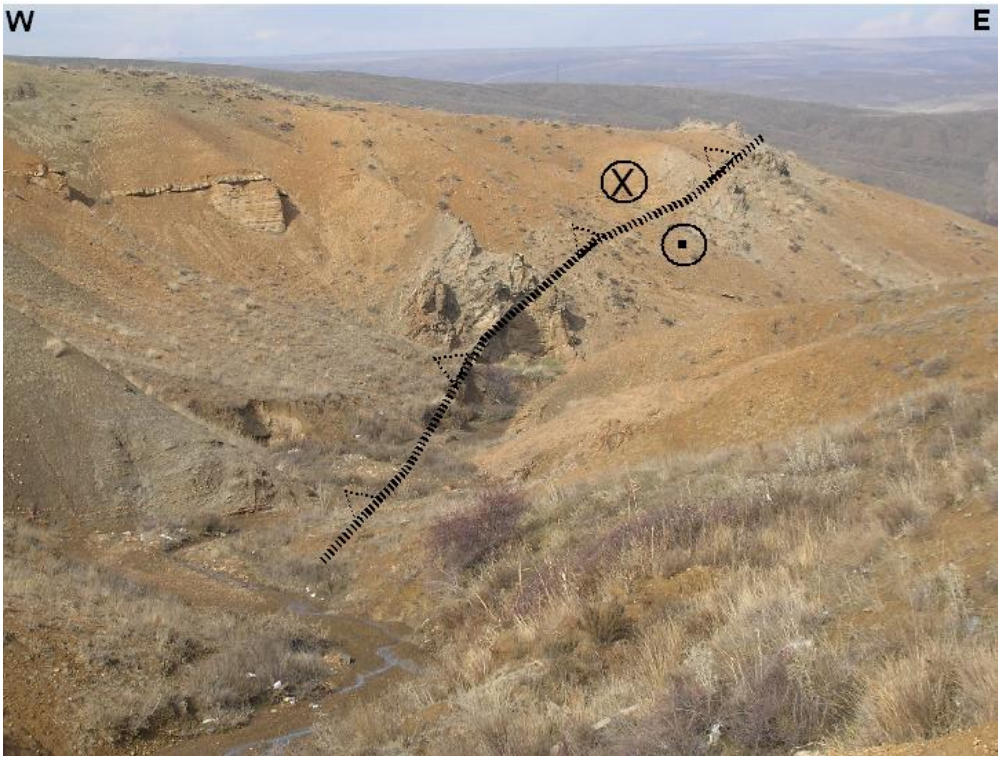

Figure 14. General view of the N25°W/50°S trending dextral strike slip fault with reverse component. Locality: NW of Belçarşak village, Ilgınözü stream.

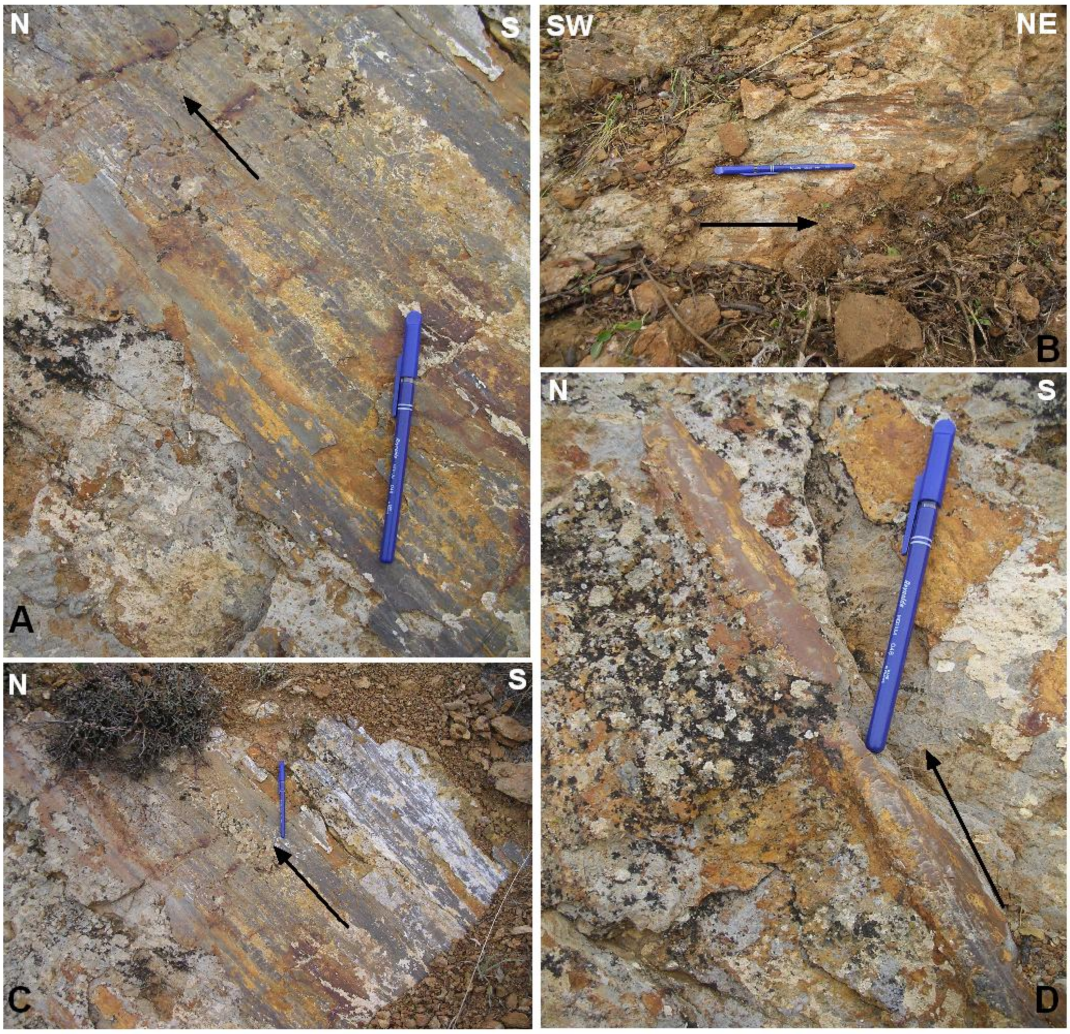

Figure 15. Slickenlines with chatter marks and grooves indicating the top to the NE reverse faulting with dextral strike slip component (A, C, D) and dextral strike slip faulting (B). Locality: Bilal'in yayla, SE of Belçarşak village.

4.1. Attitude of Bedding Planes

Totally 605 dip-strike measurements of the bedding planes from different stratigraphic levels of the Paleocene Paşadağ group were taken in the field (Figure 4, Appendix A). Beds are categorized as overturned and normal beds based on the attitude of their primary sedimentary structures, namely, flute casts, burrows, groove-scour casts, load casts and graded bedding (Figure 7, 9, 10, and 11). For the analysis of planar structure -bedding planes-, rose diagram and stereonet diagram analysis are prepared for the same age rocks and interpreted (Ragan, 1985) by using RockWorks 2009 software (www.rockware .com).

The rose diagram of all strike measurements points out broad distribution in a range of 60° (340°N - 40°N) (Figure 16). The average attitude of the beds is about N15°E. The grouping of strikes of bedding planes hardly analyzed due to this broad distribution. Therefore the bedding attitudes are analyzed based on almost the geographic position, as NW (Domain I) and SE (Domain II) of Ilgınözü stream (Figure 17). The NW domain is characterized with thick masses of conglomerates where both overturned and normal attitudes can be observed and correlated on both limbs of the structure, and faulted terrain. The SE domain is intensely faulted which may cause this broad statistical distribution of the data on the rose diagram prepared for all beds (Figure 2, 16).The geographic division also reflects the domains where there is group of the overturned or normal beddings.

The results of the analysis done with 67 beds from NW domain (Domain I) are very much consistent with the field observations (Figure 18). The results point out an average trend of N10°E. However, the rose diagram analysis done with SE domain (Domain II) data show a distributed pattern (Figure 19). The results point out an average trend of N20°E. From NW of Belçarşak village towards southeast, the attitude of the beds changes from N10°E to N20°E, except in the areas where faulted. In the faulted areas, the strikes of the beds run parallel to subparallel to the faults (Figure 2).

To understand the folding pattern, countered stereographic plot of dip and strike measurements are analyzed. As it can be seen from the geology map and lineament rose analysis diagrams, there is a clear trend in N10-20E directions. The stereographic plots are prepared separately for the northwestern part (Domain I) and southeastern part (Domain II) of the research area where the Ilgınözü stream is almost the dividing line. The results point out NNE-SSW trending single cline with NW dipping axial plane to the Domain I of the research area (Figure 20) and NNE-SSW trending asymmetrical folded pattern with NW inclined axial plane to the

Domain II (Figure 21). The presence of parallel to subparallel strikes with dipping in the same direction –NW direction- suggests that there is a single cline. The single cline –overturned syncline- is manifested with the concentration of the overturned beds to the NW of the research area.

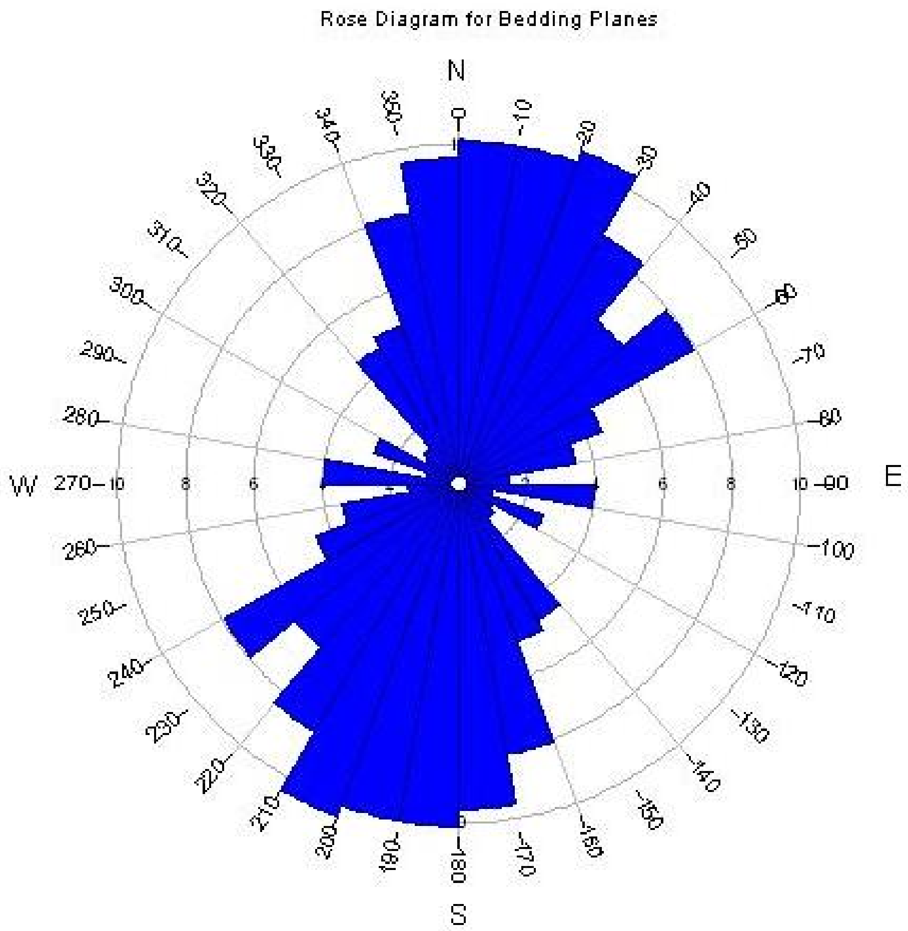

Figure 16. Rose diagram showing the strike measurements of all bedding planes (n=605).

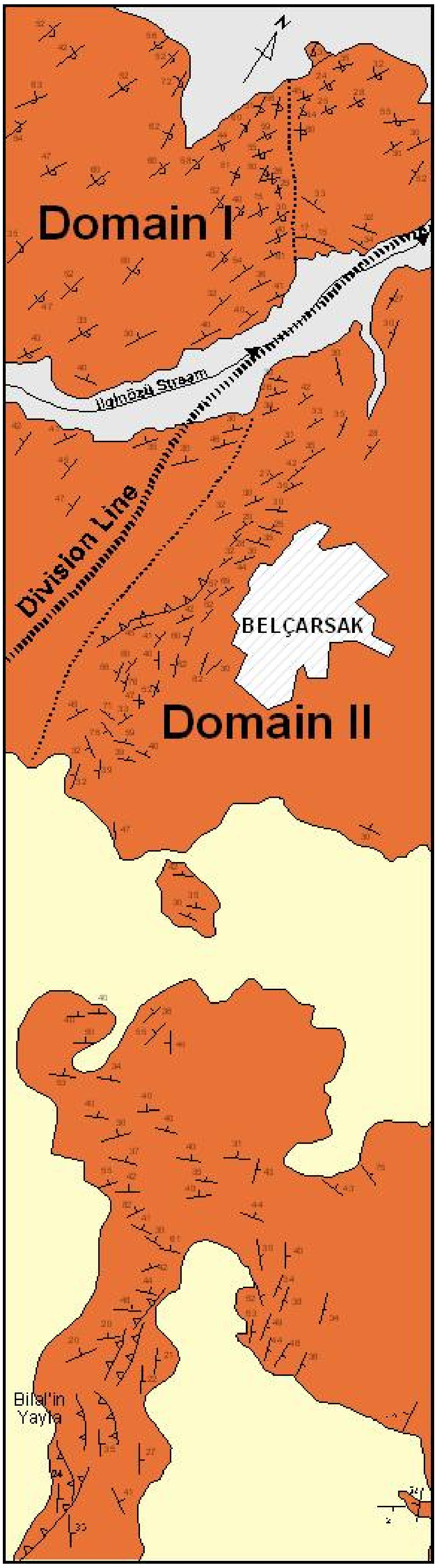

Figure 17. Domain map of the research area used in structural analysis.

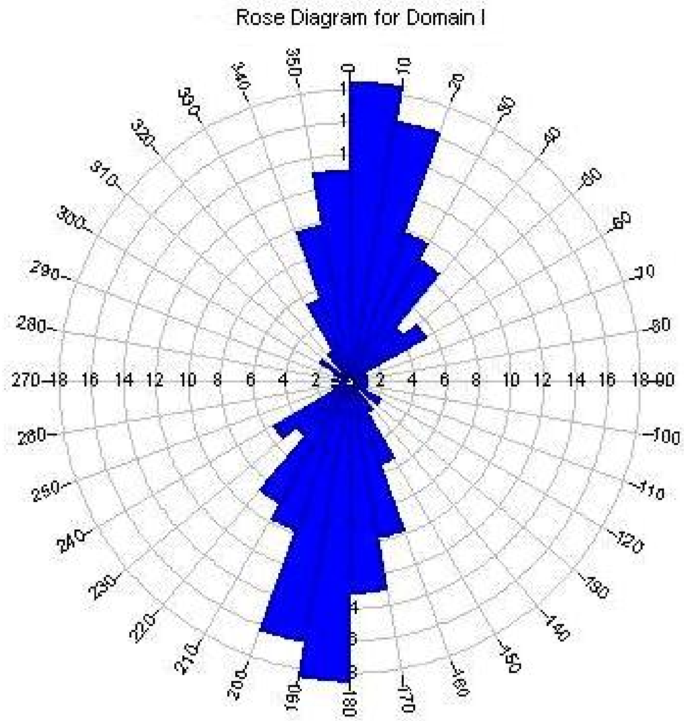

Figure 18. Rose diagram showing the strike measurements of NW domain (Domain I) bedding planes (n=51).

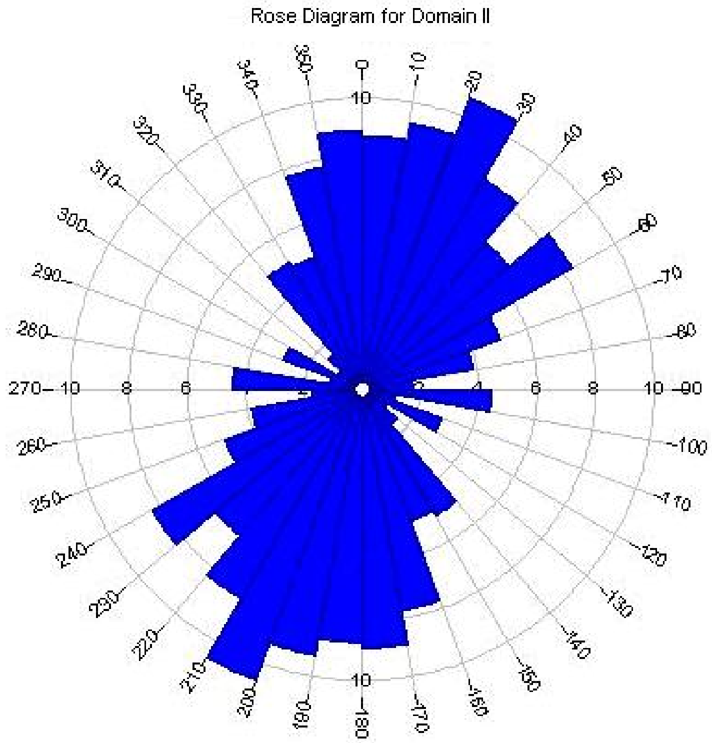

Figure 19. Rose diagram showing the strike measurements of SE domain (Domain II) bedding planes.

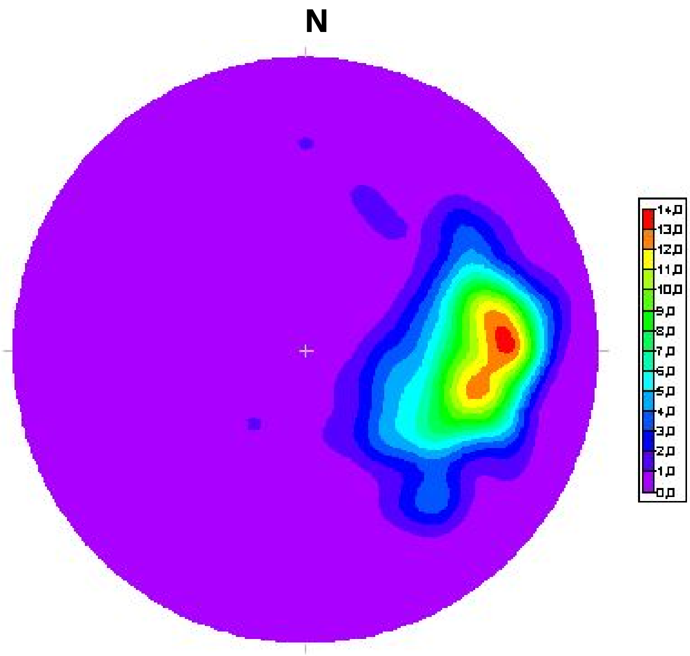

Figure 20. Stereonet Diagram for northwest part of the research area (Domain I).

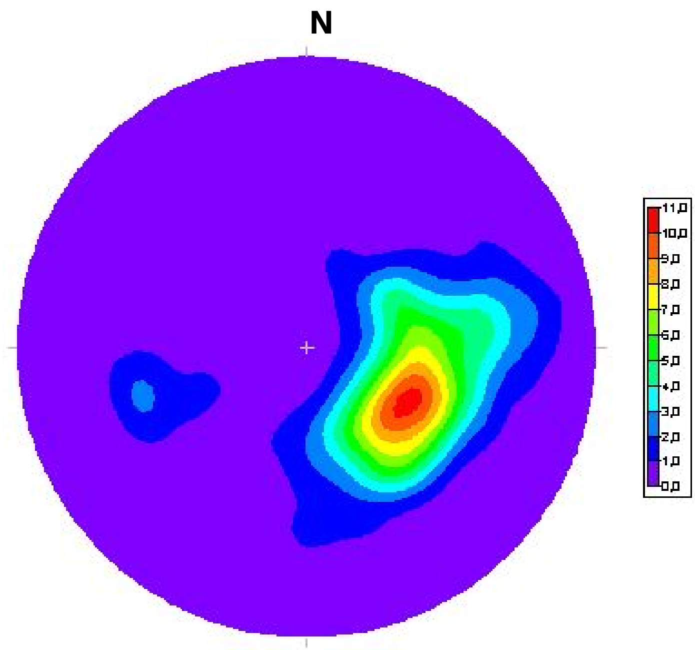

Figure 21. Stereonet Diagram for southeast part of the research area (Domain II).

4.2. Attitude of en echelon gash veins

The dip-strike measurements of calcite gash veins are measured in various points of the research area. They are mainly gathered around and NW of the Belçarşak village and Taşlık area (Figure 2). On the other hand, besides calcite veins, the en echelon trends of calcite gash veins are observed along the faulted areas (Figure 2). The veins are filled with calcite fibers and crystals (Figure 12). Some of the fibers are perpendicular to the joint walls and some are s-fibers. These might be the reflectance of extension parallel to fibers with a possible continuous shearing and slight rotation of the principal stress orientation. The gash veins are almost vertical with 2nd and 3rd pinnate calcite veins.

Total 64 measurements are taken and listed in the attached excel sheet in Appendix A. The strikes of the gash veins are analyzed. For the analysis of calcite veins, rose diagram is prepared by using RockWorks 2009 software. According to the rose diagram, their dominant trend is N15°E indicating the principal stress orientation (Figure 22).

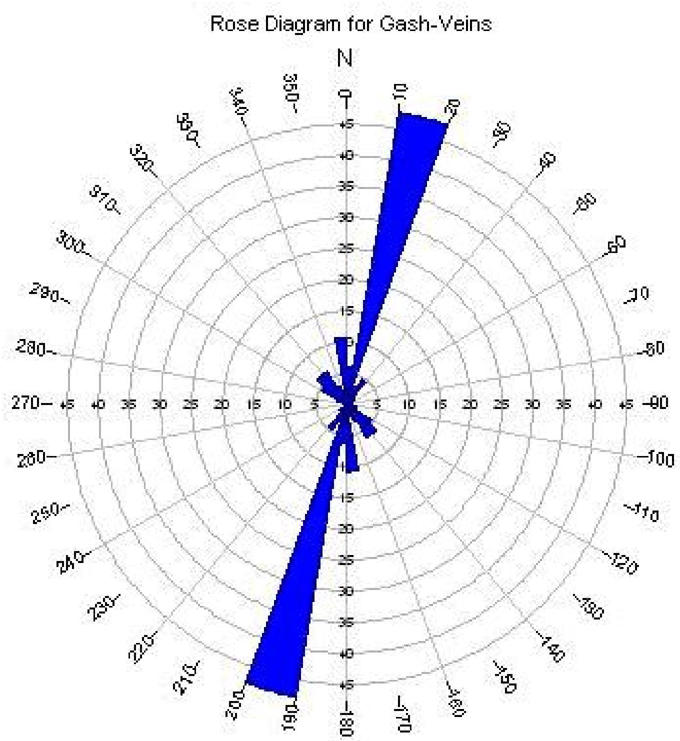

Figure 22. Rose diagram showing the strike measurements of calcite veins (n=64).

4.3. Faults

The faults are well developed with their fault plane (close-up structures) (Figure 13). Faults have a general trend in NNW-SSE orientation with offset patterns in the field and closely linked with faulted rocks like silicification, Fe-oxidation, silicified conglomerates, fault breccias, polished-striated surfaces, grooves and slickenlines (Figure 13, 14, 15 and 23). Intense hydrothermal affects are recorded along the faulted areas with reddish appearance.

Fault plane related measurements that are taken in the field are listed in Appendix B with information of dip, strike and rake measurements and sense identifications. The excel sheet contains 160 measurements where all are used in lineament analysis (RockWorks 2009) and 37 of them are with movement senses used in identifying the principal stress orientations acting on Paleocene sequence (Angelier Inversion Method).

Figure 23. Fault rocks along N trending fault. A: silicified conglomerate, B: Silicified zone and fault plane, C: silicified zone with fault breccia. Locality: Bilal'in yayla.

4.3.1 Fault Trends

Totally 160 measurements analyzed according to their strike trends. For the analysis of fault planes, rose diagram is prepared by using RockWorks 2009 software.

According to the rose diagram their dominant strike trend is found as N20°W (Figure 24). However, the faults display distributed pattern on rose diagram and ranging from N10°-40°W trends which is due to the bifurcation and offset of faults (Figure 2). The stepping pattern of the faults to the W and SW of the Belçarşak village manifests a dextral separation (Figure 2). The bifurcation pattern of faulting is clearly seen to the southwest of Belçarşak village.

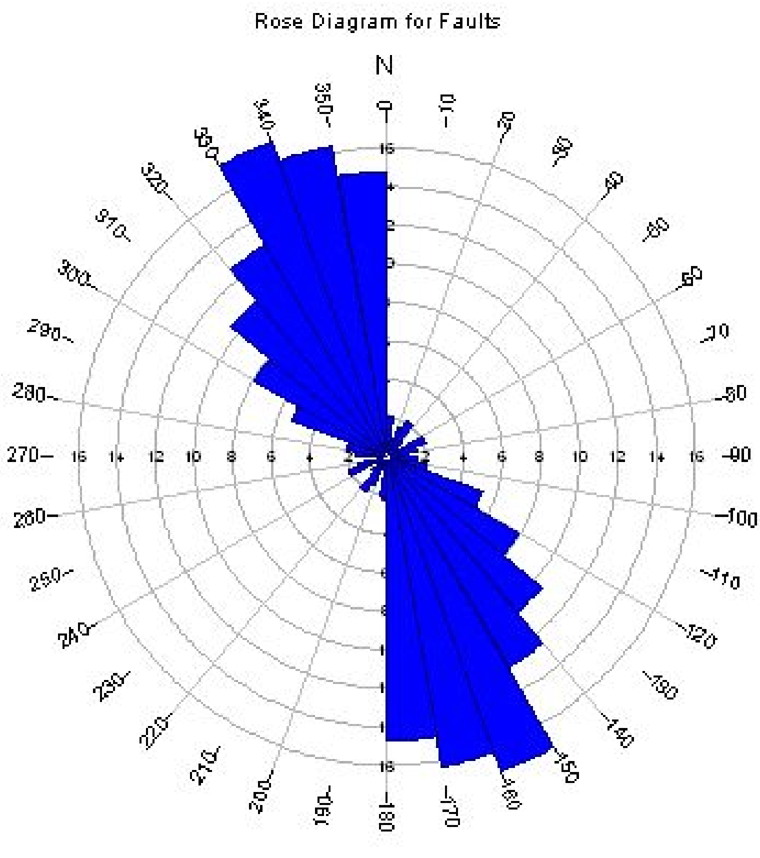

Figure 24. Rose diagram showing the strike measurements of faults (n=160).

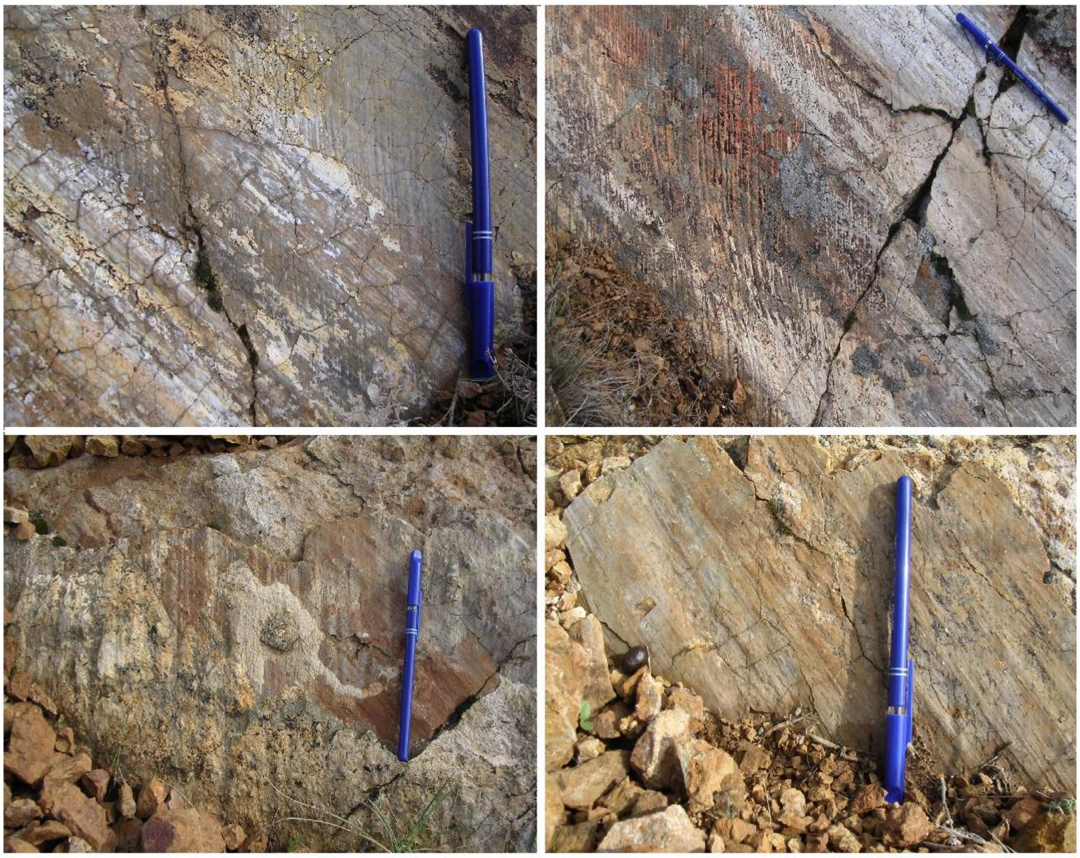

Figure 25. Overprinting of the fault slip data. The reverse fault is overprinted with dextral strike slip fault with reverse component. Locality: Bilal'in yayla.

4.3.2 Fault Stress Analysis

Total 37 slip lineation data are analyzed to differentiate the deformational phases and to find the principal stress orientations with the Tensor v.5.42 software (Angelier Inversion Method) (Angelier 1979; 1984; 1991, 1994). The software requires at least four measurements taken from each site on each fault plane and from the same age fault planes. Therefore, the data is categorized into three groups based on their field observations and rakes, as strike slip (when the rake is less than 45°), reverse and normal faults (Appendix C) (Figure 25).

4.3.2.1 Reverse faults

Totally 14 fault slip data measurements are analyzed with the Tensor v.5.42 software (Figure 26).

According to the results of the analysis, compressional principal stress (σ_1) is radial and measured to be in the NE-SW direction (Figure 26). On the other hand, the minimum stress component (σ_3) is close to the center of the circle –vertical to subvertical-. The σ_1 and σ_3 relationship simply indicates a reverse faulting.
Statistically Φ value is 0.713 where σ_1 =35°N, 10°, σ_2 =302°N, 17°, σ_3 = 153°N, 70° are measured.

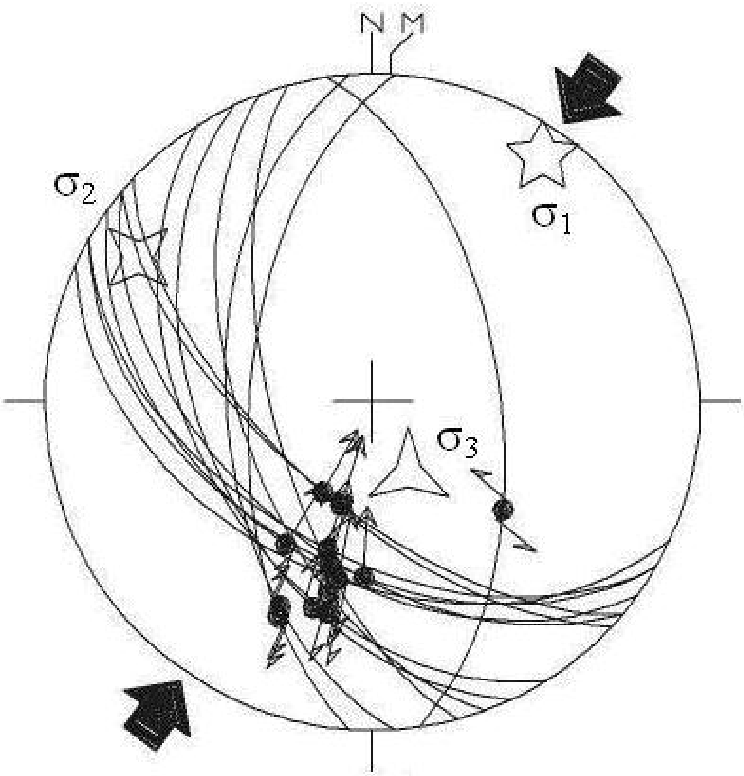

Figure 26. Fault stress analysis for reverse faults.

4.3.2.2 Strike-slip faults with reverse components

Totally 12 fault slip data measurements are analyzed by using the Tensor v.5.42 software (Figure 27). The dextral strike slip faulting with reverse components is overprinted on reverse faulting (Figure 25).

The analysis shows that principal stress component is radial –on circle- and operated almost in N-S direction (Figure 27). Intermediate and minimum stress orientations are close to the center and symmetric which is typical for strike-slip faults. However, the attitude of the σ_2 and σ_3 contributes to oblique component of the strike-slip fault which is reverse in here and may manifest a stress permutation. The analyses with the field observation support points out a dextral strike slip faulting with reverse component (Figure 27).
Statistically Φ value is 0.224, σ_1 = 185°N, 1°, σ_2 = 276°N, 38°, σ_3 = 94°N, 52° are measured.

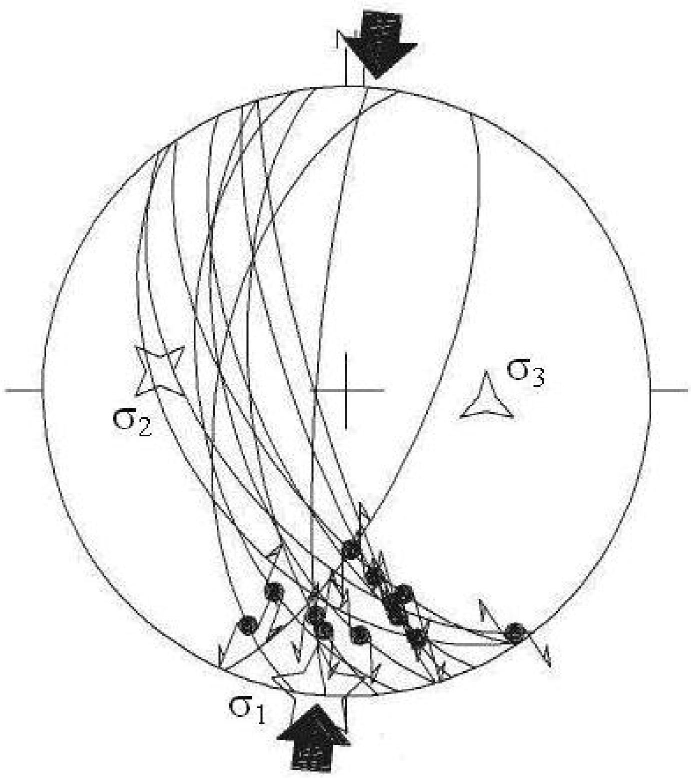

Figure 27. Fault stress analysis for strike-slip faults.

4.3.2.3 Normal faults

Totally 11 fault slip data measurements are analyzed by using the Tensor v.5.42 software (Figure 28).

The principal stress (σ_1) is at the centre of circle –perpendicular to subperpendicular orientation (Figure 28). The intermediate (σ_2) and minimum (σ_3) stress orientations are similar and concentric. Therefore, the principal stress, σ_1, is at the center indicating an extension in σ_3 direction. The extension in WNW-ESE direction is well manifested as normal faulting.

Statistically Φ value is 0.253, σ_1 = 173°N, 79°, σ_2 = 21°N, 10°, σ_3 = 290°N, 5° are measured.

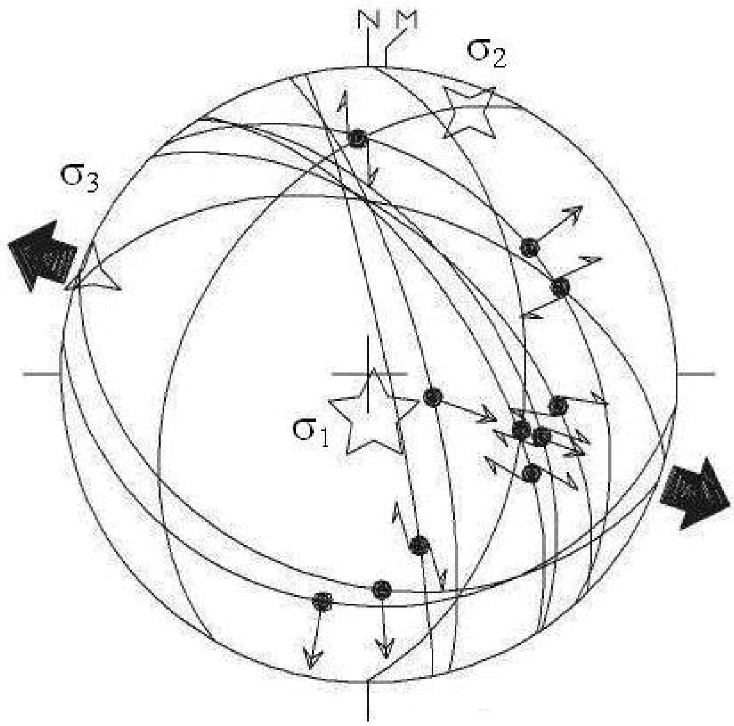

Figure 28. Fault stress analysis for normal faults.

CHAPTER 7

RESULTS

Results on the structural geology analysis based on the analysis carried out on bedding planes, en echelon gash veins and faults.

Results of the analysis carried out on bedding planes:

1. The analysis of 605 dip-strike measurements from the Paleocene section of the Paşadağ Group shows that the units have almost N15°E strikes.
2. The analysis shows a general folding trend of NNE-SSW (N10°-20°E) direction in which an overturned syncline is mapped.

The geometric and kinematic analysis done on the attitude of bedding planes points out a WNW-ESE directed compression during the formation of the folding, which lately deformed by reverse to strike-slip faulting as evidenced by field observations and slip analysis.

Results of the analysis carried out on gash veins:

1. The analysis of 64 dip-strike measurements of en echelon gash veins from the Paleocene section of the Paşadağ Group shows that the veins have a general strike of N15°E.
2. The analysis shows that attitudes of beds and gash veins have almost the same attitude. However, field observations show a very acute angular relationship between the beds and veins. There are no perpendicular relationships between the attitude of beds and veins which are expected to have tensional veins evolved during the same period. The geometric and kinematic analysis had done

on the gash veins points out an average N15°E strike. The en echelon trends of veins and field observations manifest an N-S shearing resulted in a NNE-SSW (N15°E) compressive regime in en echelon trend (Figure 29).

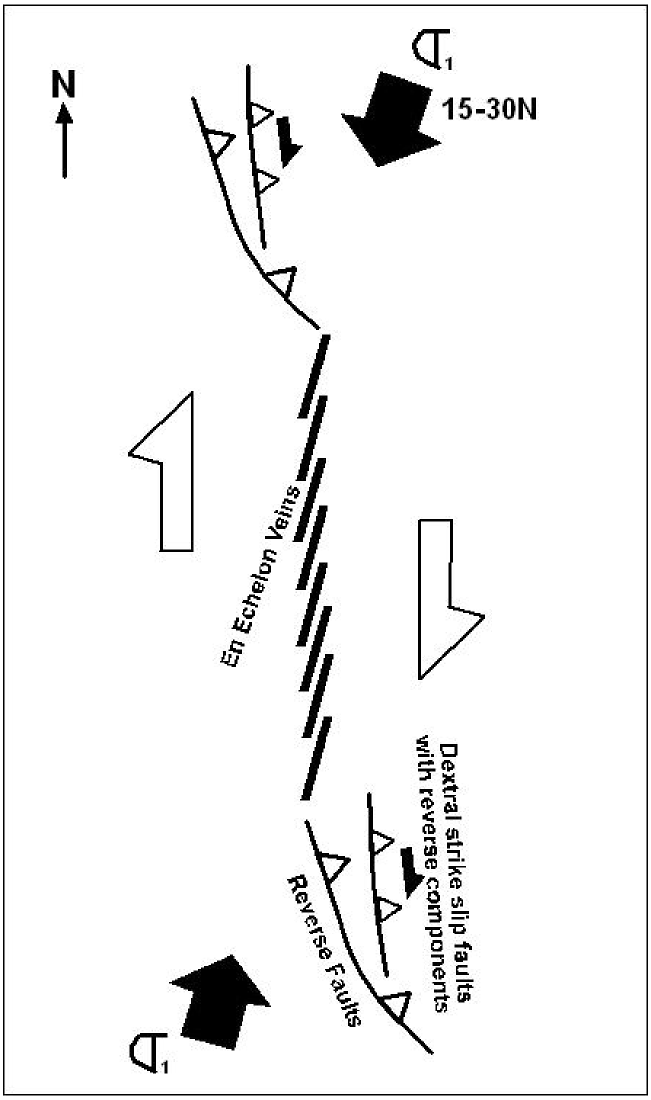

Figure 29. Fault kinematic interpretation of the post-Paleocene – pre-Oligo-Miocene structures.

Results of the analysis carried out on faults:

1. The analysis done on 160 faults by using alignments analysis pointed out NNW-SSE (N20 ° W) strikes.

2. There are two dominant groups of faults; 1) Reverse faults, 2) Dextral strike slip faults with reverse component.
3. The reverse faulting is evolved under NE-SW compression (Figure 29).
4. The dextral strike slip faulting with reverse components is evolved under almost N-S compression (Figure 29).
5. It was clearly observed that reverse faults are formed much earlier when compared with dextral strike slip faults with reverse components depending on their overprinted nature. The first motion is reverse faulting and final motion is dextral strike slip faulting with reverse component. The angular difference between the slippage is around 45-50 degrees (Figure 25).
6. The normal faulting is completely evolved under different principal stress orientation which is WNW-ESE extension during much younger period when compared with compressional structures.
7. The field observations and analysis based on the fault slip data manifest a progressive two stage of faulting under NE-SW to N-S compression during post-Paleogene – pre-Oligo-Miocene period which are followed much later by normal faulting.

To sum up, taking structural analysis on field observations into account, it can be said that the compressional regime that affected the Paleocene sequence has been most probably caused by; 1) almost WNW-ESE compression that caused folding (overturned syncline and others), 2) followed by N-S shearing (NNE-SSW en echelon gash veins) developed, and finally, 3) by NE-SW and N-S directed compressional forces that cause reverse to dextral strike slip faulting in the region. Finally normal faulting in WNW-ESE extension took place.

CHAPTER 6

DISCUSSION

The post-Paleocene deformation is well recorded in the northern tip of the Tuzgölü fault zone where neotectonic structures cross cuts them. The time constrains on the development of post-Paleocene structures will be post-Paleocene to pre-Oligo-Miocene based on regional stratigraphic configurations. Pre-Middle Eocene is an important geological time marker where different basinal configuration took place in central Anatolia. It is the time where sedimentation in basins to the south of Northern Anatolian ophiolitic accretionary (NAOA) wedge (e.g. Haymana and Tuzgölü basins) is continues during the Paleogene whereas there is a time gap between the Paleocene and Middle Eocene in northern basins of Ankara which are situated on top of the NAOA wedge (e.g. Alçı, Ankara-Orhaniye and Çankırı basins). Therefore it is believed that have a progressive tectonic development with different tectonic configurations from north to south took place since the Paleocene until the Oligo-Miocene in the central Anatolia. The Paleogene sequences are continuous sequences from Maastrichtian to the end of Eocene in Paşadağ region (Şahbaz and Köksoy 1985). Therefore age of deformation might be post-Eocene – pre- Oligo-Miocene where there is very poor age control on the Oligo-Miocene sequences.

Following the deposition of the Paleocene sequence, the WNW-ESE operating compression resulted in the development of folds (the overturned syncline to the NW of Belçarşak) (Figure 2). This compression is followed by a shearing as manifested by en echelon gash vein developments under NNE-SSW compression and the development of reverse faulting under NE-SW compression. And this progressive compressional period is continue with an almost N-S compression where dextral strike slip faulting with reverse components took place. The final tectonic evolution is the normal faulting that is development during WNW-ESE extension in the region.

Although, the number of fault slip data are not sufficient to address a clear paleostress evolution of the Paşadağ region, the fault slip data analysis and field observations have strong correlation to have conclusive results on this issue. The reliability of the results of the fault slip analysis were based on; 1) the orientation of the principal stress (σ1) and the minimum (σ3) stress orientations, and 2) the ratio Φ value. When the ratio is less than 0.4, but over 0.2, the σ1 is clear and reliable. However, when the ratio exceeded 0.6-0.7, the orientation of σ3 is clear. In reverse faulting, the minimum stress orientation is reliable and the principal stress orientation is accepted to be reliable. In the analysis, the orientation of σ3 presumed to be reliable in relation to the angular relationship between σ1 and σ2. In reverse faulting, the σ1 is radial whereas the σ3 is vertical. In both strike slip and normal faulting, the orientation of the principal stress is found reliable. In strike slip faulting, the σ1 is radial, σ2 and σ3 are symmetric and located near center which is typical for strike slip faults. In normal faulting, the σ1 is vertical and the extension is in the direction of σ3 which is both σ2 and σ3 are radial.

Contractional regime with rotational block movements continues until the end of the Late Miocene as result of the closure of the Neotehys and followed by extensional tectonic regime during post-Latest Miocene which the extensional deformational style is still under the discussion. The collision of the Kırşehir “block” to Pontide continent eased by the indentation of the Kırşehir “block” (“indentation”; Molnar and Tapponnier, 1975) and the western margin of the indenter experienced a counter clockwise rotation during Eocene (Kaymakçı 2000; Kaymakçı et al 2003). This is well conformable with the rotation of Anatolia which is evidenced as counter clockwise rotation (Rotstein 1984). During post-Eocene-Oligocene, the rotation it is calculated as 33° and 36° counter clockwise rotation. However, there is no rotation in the northeast of the terrain following the Middle

Eocene (Kaymakçı 2000). Therefore there is no indentation of the Kırşehir “block” after Middle Eocene. This may also manifest that there is no contraction after Middle Eocene in the western margin of the Kırşehir “block” where Tuzgölü basin located (Paşadağ section as a part of the Tuzgölü basin).

In central Anatolian configuration, to the north of the research area, the pre-Neogene compressional deformation is very clear as shifting from NW-SE to WNW-ESE orientation which is followed by E-W extensional period.

The NW-SE compression during the post-Late Miocene – Early Pliocene is well-recorded by various researchers and it is linked to the initiation on the North Anatolian Fault in north (Gökten et al 1988) or to the stress regime changes due to progressive collision (Koçyiğit, 1991; 1992; 2000; Koçyiğit et al 1995). There is no record of post-Pliocene N-S compression during the post-Plio-Quaternary period (Gökten et al 1988; Koçyiğit, 1991; 1992; 2000; Koçyiğit et al 1995; Özsayın et al 2005) or post-Pliocene extension in the central Anatolia which is the end of the compression in the Central Anatolia. (Rojay and Karaca, 2008) in the research area. Therefore, the compression in the research area can not linked to the Miocene compression took place in Central Anatolia.

On the other hand, the deformational analysis carried out in Aksaray-Şereflikoçhisar sector proposed the existence of a left lateral shear zone development for the period of post-Maastricthian - pre-Neogene (Derman et al 2000). The age constrains are important to address an exact deformational discussion on this issue. This might be a progressive process or two separate consecutive processes indicating an inversion in the region.

However, there is an intermittent but progressive compression in the region since post-Paleocene until the end of Miocene. Therefore, the record of compression for the Paleogene period is well conformable with the tectonic evolution of Central Anatolia.

CHAPTER 6

CONCLUSION

To conclude, the geometric and kinematic analysis done:

i) on the attitude of bedding; points out a WNW-ESE compression during the formation of the post-Paleocene folding,

ii) on the en echelon gash veins; points out an average N15°E strike. There are no perpendicular relationships between the attitude of beds and veins which are expected to have tensional veins. The en echelon trends of gash veins points out a N-S shearing on the evolution of gash veins. This shearing manifests a NNE-SSW compression,

iii) on the faults; pointed out a NE-SW compression, represented by reverse faulting which is followed by a N-S compression, represented by dextral strike slip faulting with reverse components. The final deformation is resulted from WNW-ESE extension. The deformational order of normal faulting much younger than the reverse and dextral strike slip faults.

To sum up, the Paleocene sequences are deformed under WNW-ESE directed compression which is followed by a NE-SW to N-S compression resulted in the development of a reverse to dextral strike slip faulting regime during post-Eocene - pre-Oligo-Miocene period. There is an intermittent and progressive compression in the region since post-Paleocene until the end of Miocene.

REFERENCES

Akyürek, B., Bilginer, E., Akbaş, B., Hepşen, N., Pehlivan, Ş., Sunu, O., Soysal, Y., Dağer, Z., Çatal, E., Sözeri, B., Yıldırım, H., and Hakyemez, Y., 1984. Ankara-Elmadağ-Kalecik dolayının temel jeoloji özellikleri. Jeoloji Mühendisliği,20, 31-46.

Angelier, J., 1979. Determination of the mean principal directions of stresses for a given fault population. Tectonophysics, 56, T17−T26.

Angelier, J., 1984. Tectonic analysis of fault slip data sets. Journal of Geophysical Research, 80, 5835–5848.

Angelier, J., 1991. Inversion of field data in fault tectonics to obtain regional stress. III: A new rapid direct inversion method by analytical means. Geophysical Journal International, 103, 63–76.

Angelier, J., 1994. Fault slip analysis and paleostress reconstruction. In: Hancock, P.L. (ed.) Continental deformation. Pergamon Press, Oxford. 53-100.

Arıkan, Y., 1975. Tuz gölü havzasının jeolojisi ve petrol imkanları. MTA Bulletin, 85, 17-38.

Bailey, E. B., and Mc.Callien, W. J., 1950. The Ankara Melange and The Anatolian Thrust. MTA Bulletin, 40, 12-22.

Brinkmann, R., 1976. Geology of Turkey. Elsevier Sci. Publ. Company, 158p.

Chaput, E., 1936. Voyages d'études géologiques et géomorphologiques en Turquie. Mém. Inst. Françaiş D'Archaéo. İstanbul, II, 312 p.

Çemen, I., Göncüoğlu, M.C., and Dirik, K., 1999. Structural evolution of the Tuzgölü basin in central Anatolia, Turkey. Journal of Geology, 107, 693-706.

Çiner A., 1993. Geology of Haymana Basin (U. Cretaceous – M. Eocene); Central Anatolia, Turkey. 6th International Meeting and Training School on IGCP Project 269, Middle East Technical University, Field Trip Guide Book, 21 p.

Dellaloğlu, A. A. and Aksu, R., 1984. Kulu, Şereflikoçhisar, Aksaray dolayının jeolo-jisi ve petrol olanakları. TPAO Report 2020.

Dellaloğlu, A.A., Tüysüz, O., Kaya, O.H., and Harput, B., 1992. Kalecik (Ankara)-Eldivan-Yapraklı (Çankırı)- İskilip (Çorum) ve Devrez Çayı arasindaki alanın jeolojisi ve petrol olanakları. TPAO Report 3194.

Derman, S., 1980. Tuzgölü doğu ve kuzeyinin jeolojisi. TPAO Report 1512.

Derman, S., Rojay, B., Güney, H., and Yıldız, M., 2003. Şereflikoçhisar-Aksaray fay zonunun evrimi hakkında yeni sedimentolojik veriler. Haymana-Tuzgölü-Ulukışla Basenleri Uygulamalı Çalışması, Proccedings, 47-70.

Dirik, K. and Göncüoğlu, M. C., 1996. Neotectonic characteristics of Central Anatolia. Int. Geology Review, 38, 807- 817.

Dirik, K. and Erol, O., 2000. Tuzgölü ve civarının tektonomorfolojik evrimi, Orta Anadolu, Türkiye. Haymana-Tuzgölü-Ulukışla Basenleri Uygulamalı Çalışma, Prooceedings, 27−46.

İlhan, E., 1976. Türkiye Jeolojisi. ODTÜ Mühendislik Fakültesi Publication No: 51. 239p.

Egeran, N. and Lahn, E., 1951. Kuzey ve Orta Anadolu'nun tektonik durumu hakkında not. MTA Bulletin, 41, 23-34.

Erol, O., 1961. Ankara bölgesinin tektonik gelişmesi. TJK Bulletin, VII/1, 57-85.

Erol, O., 1993. Ankara yöresinin jeomorfolojik gelişimi. A. Suat Erk Geology Symposium, Proceedings, 25−35.

Egeran, N. and Lahn, E., 1951. Kuzey ve Orta Anadolu'nun tektonik durumu hakkında not. MTA Bulletin, 41, 23-28.

Gökten, E., Kazancı, N., and Acar, Ş., 1988. Ankara kuzeybatısında (Bağlum-Kazan arası) Geç Kretase-Pliyosen serilerinin stratigrafisi ve tektoniği. MTA Bulletin, 108, 69-81.

Göncüoğlu, M. C., Dirik, K., and Kozlu, H., 1997. Pre-Alpine and Alpine terranes in Turkey: explanatory notes to the terrane map of Turkey. In: D. Papanikolaou and F.P. Sassi, Editors, IGCP Project no 276; Paleozoic domains and their alpidic evolution in the Tethys, Annales Géologiques des Pays Helléniques, 37**,** 515–536.

Göncüoğlu, M.C., Erler, A., Toprak, V., Yalınız, K., Olgun, E., and Rojay, B., 1992. Orta Anadolu masifinin batı bölümünün jeolojisi. Bölüm 2; Orta Kesim, TPAO Report 2909.

Görür, N. and Derman, A. S., 1978. Stratigraphic and tectonic analysis of the Tuzgölü-Haymana basins. TPAO Report 1514.

Görür N., Tüysüz O., and Şengör, A. M. C., 1998. Tectonic evolution of the central Anatolian basins. International Geology Review, 40, 831-850.

Görür, N., Oktay, F., Seymen, I., and Şengör, A.M.C., 1984. Paleotectonic evolution of Tuzgölü basin complex, central Turkey, In Dixon, J.E., and Robertson, A.H.F., eds. The geological evolution of the eastern Mediterranean Spec. Publ. Geol. Soc., 17, 81-96.

Kaymakcı, N., 2000. Tectono-stratigraphical Evolution of the Çankırı Basin (Central Anatolia, Turkey). PhD Thesis, Universiteit Utrecht, Utrecht.

Kaymakcı, N., White, S.H., and VanDijk, P.M., 2003. Kinematic and structural development of the Çankırı Basin (Central Anatolia, Turkey): a paleostress inversion study. Tectonophysics, 364, 85−113.

Ketin, I., 1966. Anadolu'nun tektonik birlikleri. MTA Bulletin, 66, 20-34.

Ketin, İ., 1983. Türkiye Jeolojisine Genel Bir Bakış. İTÜ Kütüphanesi, Sayı: 1259, 591p.

Koçyiğit, A., 1991. Changing stress orientation in progressive intracontinental deformation as indicated by the neotectonics of the Ankara region (NW Central Anatolia). TPJD Bulletin, 3, 43−55.

Koçyiğit, A., 1992. Southward-vergent imbricate thrust zone in Yuvaköy: A record of the latest compressional event related to the collisional tectonic regime in Ankara-Erzincan Suture Zone. TPJD Bulletin 4, 111−118.

Koçyiğit, A., 2000. Orta Anadolu'nun genel neotektonik özellikleri ve depremselliği. Haymana-Tuzgölü-Ulukışla Basenleri Uygulamalı Çalışması, Proccedings, 1−26.

Koçyiğit, A. and Lünel, A.T., 1987. Geology and tectonic setting of Alcı region, Ankara. METU Journal of Pure and Applied Sciences, 20, 1, 35-57.

Koçyiğit, A., Özkan, S., and Rojay, B. 1988. Examples from the forearc basin remnants at the active margin of northern Neo-Tethys; development and emplacement ages of the Anatolian Nappe, Turkey. METU Journal of Pure and Applied Science, 21, 183−210.

Koçyiğit, A., Türkmenoğlu, A., Beyhan, A., Kaymakçı, N., and Akyol, E., 1995, Post-Collisional Tectonics of Eskişehir-Ankara-Çankırı Segment of İzmir-Ankara-Erzincan Suture Zone: Ankara Orogenic Phase. TPJD Bulletin, 6/1, 69-86.

Lokman, K. and Lahn, E., 1946. Haymana bölgesi jeolojisi. MTA Bulletin, 36, 292-300.

Molnar, P. and Tapponnier, P., 1975. Cenozoic tectonics of Asia: Effects of a continental collision. Science, 74, 419-462.

Norman, T., 1972. Ankara Yahşıhan bölgesinde Üst Kretase-Alt Tersiyer stratigrafisi. TKJ Bulletin, 15, 180-276.

Oktay, F.Y. and Dellaloğlu, A.A., 1991. Tuzgölü havzası (Orta Anadolu) stratigrafisi üzerine yeni görüşler. 7.Petrol kongresi, Bildiriler, 312-321.

Özsayın, E., Yürür, T., and Dirik, K., 2005. Yuva ve Yakacık köyleri (Ankara kuzeybatısı, İç Anadolu) çivarındaki Üst Kretase ofiyolitik karmaşığı ile Miyosen birimlerinin dokunak ilişkileri ile ilgili yeni gözlemler. Yerbilimleri 26, 55−59.

Ragan, D. M., 1985. Structural geology: An introduction to geometrical techniques. 3rd edition, John Wiley and Sons, Inc., 393p.

Rojay, B. and Karaca A., 2008. Post-Miocene deformation in south of the Galatian volcanic province, NW of Central Anatolia (Turkey). T. Jour. of Earth Sci., 17, 653-672.

Rotstein, Y., 1984. Counterclockwise rotation of the Anatolian Block. Tectonophysics, 108, 71−91.

Şahbaz, A. and Köksoy, M., 1985. Stratigraphic and Tectonic Study of the Paleogene Sedimentary Sequence of the Pasadağ (N of Tuz Gölü). Bulletin of Earth Sciences Application and Research Centre of Hacettepe University, 12, 1-17.

Şengör, A.M.C., 1980. Türkiye'nin Neotektoniğinin Esasları. TJK Konferans serisi, 2.

Şengör, A. M. C. and Yılmaz, Y. 1981. Tethyan Evolution of Turkey: A Plate Tectonic Approach. Tectonophysics, 75, 181-241.

Şengör, A., Görür, N., and Saroğlu, F., 1985. Strike-Slip Faultinf and Related Basin Formation In Zones of Tectonic Escape: Turkey as case study, in Bittle, K.T. and Christe-Blick, N. (eds.), strike slip formation and sedimentation. Soc. Economic Paleontologist and Mineralogists, Special Publication, 37, 227-265.

Toprak, V. and Göncüoğlu, M. C., 1993. Tectonic control on the development of Neogene-Quaternary Central Anatolian volcanic province, Turkey. Geological Journal., 28, 357-369.

Turgut, S., 1978. Tuzgölü havzasının stratigrafik ve cökelsel gelişmesi. TPAO Report 1227.

Uygun, A., 1981, Tuzgölü havzasının jeolojisi, evaporit oluşumları ve hidrokarbon olanakları. TJK İç Anadolu sempozyumu, 66-71.

Ünalan, G., Yüksel, V., Tekeli, T., Gönenç, O., Seyirt, Z., and Hüseyin, S., 1976. Haymana-Polatlı yöresinin (Güneybatı Ankara) Üst Kretase-Alt Tersiyer stratigrafisi ve paleocoğrafik evrimi. TJK Bulletin, 19, 159-176.

Yüksel, S., 1970. Etude geologique de la region d'Haymana (Turquie Centrale). These Univ. Nancy, 179p.

APPENDIX A

Table A. Gash vein and Bedding plane

Site number	Gash vein		Bedding plane	
	Strike	Dip	Strike	Dip
1			290	45N
2			295	32N
3			144	20S
4	190	90	158	15S
5	310	90	338	19N
6			328	28N
7			222	22N
8	200	90	215	25N
9	305	90	203	40N
10	288	90	230	69N
11			190	22N
12			230	10N
13			250	22N
14			250	28N
15	210	90	238	30N
16	194	90	270	36N
17	192	90	270	36N
18	194	90	290	28N
19	192	90	290	28N
20	192	90	270	28N
21			220	32N
22			228	22N
23			0	34E
24	190	90	216	36N
25	190	90	216	36N
26	185	90	216	36N
27	185	90	216	36N
28			216	42N

Table A. cont'd.

Site number	Gash vein		Bedding plane	
	Strike	Dip	Strike	Dip
29			212	40N
30			180	22W
31			180	20W
32			180	26W
33			190	32N
34			140	25S
35	180	90	170	30S
36	195	90	170	30S
37			190	34N
38			140	22S
39	180	90	146	28S
40	180	90	146	28S
41	180	90	146	28S
42	180	90	146	28S
43	180	90	146	28S
44	180	90	146	28S
45	180	90	146	28S
46	180	90	146	28S
47	355	90	146	28S
48	355	90	146	28S
49	190	90	307	42N
50	190	90	307	42N
51	180	90	307	42N
52	180	90	307	42N
53	0	60E	160	28S
54	0	45E	160	28S
55			180	40W
56			170	32S
57			170	32S
58			175	42S
59			180	34W
60			115	24S
61			180	32W

Table A. cont'd.

Site number	Gash vein		Bedding plane	
	Strike	Dip	Strike	Dip
62			180	24W
63			90	22S
64			210	30N
65			180	32W
66	270	60N	170	40S
67	0	60E	170	40S
68			355	30N
69			160	30S
70			190	35N
71			180	30W
72			200	30N
73			170	32S
74			180	55W
75			10	62S
76			170	42S
77			170	42S
78			180	48W
79			170	51S
80			170	48S
81			190	51N
82			200	50N
83			210	70N
84			190	49N
85			190	46N
86			218	30N
87			180	38W
88			230	46N
89			270	66N
90			240	44N
91			310	80N
92			245	46N
93			170	40S
94			180	38W

Table A. cont'd.

Site number	Gash vein		Bedding plane	
	Strike	Dip	Strike	Dip
95			192	40N
96			160	42S
97			180	32W
98			180	36W
99			270	54N
100			245	38N
101			280	51N
102			290	80N
103			90	41S
104			195	30N
105			212	42N
106			200	40N
107	EW	90	200	40N
108	EW	90	200	40N
109	EW	90	200	40N
110			210	38N
111			190	40N
112			200	46N
113			225	30N
114			204	26N
115			230	32N
116			190	54N
117			200	64N
118			220	35N
119			210	28N
120	N30E	80S	210	28N
121			240	40N
122			204	55N
123			220	34N
124			190	46N
125			170	31S
126			180	42W
127			180	24W

Table A. cont'd

Site number	Gash vein		Bedding plane	
	Strike	Dip	Strike	Dip
128			180	21W
129			204	40N
130	N24E	87S	180	26W
131			170	35S
132	N40E	90	200	35N
133			200	20N
134			230	30N
135			240	45N
136			200	29N
137			230	20N
138			270	18N
139			220	50N
140			240	15N
141			325	53N
142			340	50N
143			280	26N
144	N25W	90	224	35N
145			205	40N
146			210	45N
147			230	45N
148			230	55N
149			190	32N
150			270	87N
151	N30E	90	270	72N
152			240	40N
153			240	48N
154			235	45N
155			230	44N
156			230	44N
157	N10W	90	220	44N
158			254	54N
159			254	67N
160			116	54S

Table A. cont'd

Site number	Gash vein		Bedding plane	
	Strike	Dip	Strike	Dip
161			250	66N
162			290	90
163			260	52N
164			230	46N
165			210	35N
166			70	72S
167			200	45N
168			205	28N
169			200	50N
170			200	38N
171			210	40N
172			200	29N
173			230	33N
174			230	50N
175			230	42N
176			230	44N
177			232	52N
178			210	50N
179			270	60N
180			50	50S
181			110	30S
182			70	50S
183			270	66N
184			50	31S
185			260	50N
186			250	60N
187			200	52N
188			90	50S
189			110	20S
190			210	40N
191			180	50W
192			220	30N
193			230	63N

Table A. cont'd

Site number	Gash vein		Bedding plane	
	Strike	Dip	Strike	Dip
194			146	34S
195			190	35N
196			270	35N
197			270	53N
198			155	14S
199			170	46S
200			220	25N
201			230	32N
202			240	26N
203			240	25N
204			250	20N
205			220	30N
206			240	25N
207			220	30N
208			240	44N
209			0	18E
210			250	34N
211			70	45S
212			10	50S
213			350	50N
214			325	45N
215			180	42W
216			230	52N
217			250	52N
218			250	26N
219			230	45N
220			220	45N
221			270	42N
222			200	30N
223			160	25S
224			250	32N
225			290	20N
226			270	52N

Table A. cont'd

Site number	Gash vein		Bedding plane	
	Strike	Dip	Strike	Dip
227			260	45N
228			160	40S
229			180	30W
230			270	30N
231			180	40W
232			160	30S
233	NS	90	165	30S
234	N10W	90	165	30S
235			190	22N
236			170	06S
237	N10W	60S	70	06S
238			210	20N
239			240	25N
240			220	30N
241			230	22N
242			260	40N
243	N60W	90	249	28N
244			260	40N
245			250	25N
246			200	20N
247			190	30N
248			200	20N
249			190	40N
250			220	20N
251			340	15N
252			252	25N
253			180	58W
254			230	57N
255			170	57S
256	N50E	70S	180	60W
257			350	60N
258			350	57N
259			350	52N

Table A cont'd

Site number	Gash vein		Bedding plane	
	Strike	Dip	Strike	Dip
260			180	50W
261			170	60S
262			170	57S
263			180	64W
264			170	52S
265			140	60S
266			170	60S
267			180	55W
268			180	63W
269			150	48W
270			190	25N
271			230	40N
272			50	40S
273			200	36N
274			0	60E
275			110	30S
276			155	30S
277			155	32S
278			160	33S
279			220	20N
280			90	34S
281			110	28S
282			170	64S
283			165	62S
284			180	70W
285			190	45N
286			160	40S
287			0	40E
288			10	20S
289			180	35W
290			90	47S
291			140	40S
292			130	52S

Table A. cont'd

Site number	Gash vein		Bedding plane	
	Strike	Dip	Strike	Dip
293			125	42S
294			160	22S
295			232	42N
296			220	48N
297			220	42N
298			180	56W
299			170	75S
300			170	72S
301			180	60W
302			162	68S
303			150	55S
304			150	66S
305			140	55S
306			180	45W
307			216	45N
308			180	52W
309			170	52S
310			160	60S
311			165	55S
312			150	44S
313			160	52S
314			150	56S
315			180	45W
316			170	52S
317			240	60S
318			180	50W
319			170	60S
320			180	58W
321			170	62S
322			147	40S
323			151	42S
324			180	65W
325			170	40S

Table A. cont'd

Site number	Gash vein		Bedding plane	
	Strike	Dip	Strike	Dip
326			170	55S
327			152	65S
328			155	55S
329			168	52S
330			160	64S
331			166	62S
332			315	82N
333			10	42S
334			170	48S
335			168	46S
336			142	60S
337			162	50S
338			134	64S
339			164	66S
340			150	40S
341			144	42S
342			175	70S
343			175	68S
344			150	48S
345			152	60S
346			185	52N
347			180	51W
348			175	52S
349			170	72S
350			180	55W
351			180	35W
352			190	31N
353			198	22N
354			164	54SW
355			180	25W
356			162	30SW
357			168	55SW
358			206	55N

Table A. cont’d

Site number	Gash vein		Bedding plane	
	Strike	Dip	Strike	Dip
359			200	50N
360			10	54SW
361	N50W	90	155	60S
362			198	48N
363			214	46N
364			200	59N
365			200	55N
366			200	51N
367			348	50N
368			350	54N
369			180	60W
370			192	58N
371			200	44N
372			190	32N
373			170	45S
374			215	45N
375			210	40W
376			210	50N
377			218	44N
378	N60W	66N	210	46N
379			162	48S
380			328	26N
381			280	20N
382			305	25N
383			140	18S
384			80	35S
385			200	50N
386			110	25S
387			162	46S
388			165	55S
389			165	66S
390			210	50N
391			205	45N

Table A. cont'd

Site number	Gash vein		Bedding plane	
	Strike	Dip	Strike	Dip
392			205	64N
393			168	51S
394			180	60W
395			190	61N
396			10	51S
397			210	15N
398			155	32S
399			190	62N
400			180	78W
401			180	40W
402			190	60N
403			200	60N
404			190	24N
405			165	34S
406			213	18N
407			192	40N
408			170	50S
409			200	40N
410			208	61N
411			195	50N
412			180	44W
413			195	30N
414			177	34S
415			170	46S
416			192	50N
417			205	42N
418			192	43N
419			210	42N
420			202	32N
421			192	40N
422			204	12N
423			220	40N
424			193	33N

Table A. cont'd

Site number	Gash vein		Bedding plane	
	Strike	Dip	Strike	Dip
425			202	31N
426			205	34N
427			204	35N
428			230	42N
429			210	33N
430			230	35N
431			245	30N
432			245	25N
433			248	30N
434			250	25N
435			250	22N
436			230	38N
437			230	29N
438			225	31N
439	N10W	90	220	27N
440			210	30N
441			210	27N
442			216	29N
443			24	80S
444	N12W	90	345	30N
445	N12E	56S	230	30N
446			200	35N
447			200	34N
448	N15E	90	202	31N
449			200	32N
450			220	40N
451	NS	25E	190	50N
452			202	34N
453	N50W	90	200	42N
454	N40W	90	200	42N
455			217	31N
456			260	24N
457	NS	90	225	26N

Table A. cont'd

Site number	Gash vein		Bedding plane	
	Strike	Dip	Strike	Dip
458			230	32N
459			205	35N
460			215	44N
461			235	41N
462			200	32N
463			205	32N
464	N37W	90	208	30N
465			222	31N
466			195	42N
467			200	28N
468			230	27N
469			219	25N
470			213	32N
471			211	27N
472			207	20N
473			225	30N
474			197	31N
475			212	27N
476			235	35N
477			211	32N
478			192	47N
479			190	69N
480			191	52N
481	NS	72W	175	67S
482			210	31N
483			192	50N
484			215	45N
485			192	52N
486			210	42N
487			210	41N
488			190	90N
489			192	42N
490	N62W	90	192	52N

Table A. cont'd

Site number	Gash vein		Bedding plane	
	Strike	Dip	Strike	Dip
491			192	41N
492			195	39N
493			217	67N
494			170	67S
495			180	55W
496			170	37S
497			180	65W
498			172	62S
499			332	52N
500			170	28S
501			220	75N
502			192	35N
503			172	75S
504			169	71S
505			180	63W
506			198	56N
507			195	71N
508			192	30N
509	N30W	90	168	50S
510			165	81S
511			175	52S
512			180	76W
513			175	50S
514			159	47S
515			345	90E
516			240	39N
517			348	90E
518			170	79S
519			180	66W
520			320	75N
521			222	40N
522			230	32N
523			221	39N

Table A. cont'd

Site number	Gash vein		Bedding plane	
	Strike	Dip	Strike	Dip
524			224	28N
525			245	32N
526			135	76S
527			290	71N
528			260	51N
529			109	51S
530			250	59N
531			249	41N
532			241	39N
533			205	39N
534			270	53N
535			180	45W
536			90	60S
537			120	59N
538			100	51S
539			150	60S
540			138	32S
541			180	32W
542			165	39S
543			110	47S
544			223	53N
545			230	30N
546			233	33N
547			235	34N
548			175	36S
549			168	55S
550			130	40S
551			210	30N
552			230	40N
553			230	37N
554			225	55N
555			210	45N
556			207	37N

Table A. cont'd

Site number	Gash vein		Bedding plane	
	Strike	Dip	Strike	Dip
557			240	50N
558			240	36N
559			260	30N
560			240	36N
561			223	45N
562			221	42N
563			190	82N
564			270	40N
565			250	41N
566			230	20N
567			270	31N
568			216	90N
569			240	31N
570			220	41N
571			208	42N
572			230	61N
573			190	69N
574			165	56S
575			164	22S
576			242	44N
577			350	46N
578			348	48N
579			336	36N
580			336	35N
581			346	48N
582			342	44N
583			339	49N
584			328	36N
585			335	52N
586			338	53N
587			339	51N
588			350	44N
589			329	36N

Table A. cont'd

Site number	Gash vein		Bedding plane	
	Strike	Dip	Strike	Dip
590			334	52N
591			338	59N
592			236	44N
593			338	43N
594			223	31N
595			216	55N
596			230	42N
597			222	35N
598	N42W	42S	180	55W
599			25	42S
600			342	28N
601			108	14S
602			133	18S
603			192	22N
604			202	55N
605			220	15N

APPENDIX B

Table B. Fault.

Site number	Strike	Dip	Rake	Sense
1	170	42SW	46S	
2	165	65SW	50SW	R DS
3	160	57SW	50S	R DS
4	170	50SW	42S	R DS
5	163	58SW	25S	R DS
6	174	64SW	25S	R DS
7	174	64SW	0	
8	180	62W	37S	
9	180	60W	39S	
10	160	76S	40S	R DS
11	154	68S	44S	
12	4	59NW	35S	R DS
13	130	40S	80NW	
14	160	65S	48S	
15	180	62W	35S	
16	176	62SW	40S	
17	176	55SW	50S	
18	176	55SW	90	
19	135	50SW	55S	
20	130	65S	80S	R DS
21	120	52S	82S	R DS
22	122	62S	85S	
23	133	65S	84S	R DS
24	176	53SW	42S	R DS
25	126	52SW	78S	
26	170	77SW	43SW	

Table B. cont'd

Site number	Strike	Dip	Rake	Sense
27	170	47SW	42S	
28	170	50SW	40S	
29	162	46SW	48S	
30	150	37SW	54S	
31	176	54SW	38S	
32	163	56SW	30S	
33	105	54SW	60W	
34	116	79SW	42W	
35	77	75SE	47W	
36	276	87N	63NW	
37	180	65W	40S	
38	165	52SW	42SW	
39	158	45SW	48SW	
40	175	85SW	60SW	
41	333	40NE		
42	318	34NE	87E	N
43	1	48E	77SE	N
44	1	48E	60NE	
45	35	73SE	50E	
46	330	35NE		
47	96	26S	85SW	N DS
48	110	33SW	70SE	N SS
49	125	43SW	55S	
50	142	52SW	54S	
51	142	52SW	05NE	DS
52	130	44SW	56SE	
53	156	58SW	39S	
54	286	44NE	50E	N DS
55	146	80SW	50S	
56	156	54SW	40S	
57	150	50SW	42S	
58	140	48SW	52S	
59	150	56SW	45S	

Table B. cont'd

Site number	Strike	Dip	Rake	Sense
60	154	56SW	42S	
61	164	75SW	40S	
62	146	63SW	36S	R DS
63	148	45SW	54S	
64	156	59SW	45S	
65	326	55NE	52E	N DS
66	315	53NE	50E	N DS
67	327	61NE	45SE	N DS
68	164	79SW	25S	
69	157	60SW	35S	
70	158	70SW	35S	
71	155	51SW	32S	
72	155	66SW	28S	R DS
73	160	60SW	31S	
74	140	68SW	48S	
75	120	45SW	90	
76	118	53SW		
77	110	49SW	90	
78	145	43SW	25S	R DS
79	120	40SW	90	
80	115	45SW	80S	R
81	120	49SW	80S	R
82	115	52SW	90S	
83	126	48SW	87S	R
84	108	55SW	90S	
85	125	42SW	90S	
86	110	63SW	90S	
87	123	63SW	90S	
88	90	65S	84SW	
89	120	47SW	90	
90	133	47SW	78S	
91	130	54SW	68S	
92	130	58SW	75S	

Table B. cont'd

Site number	Strike	Dip	Rake	Sense
93	132	64SW	77S	
94	140	80SW	40S	
95	140	55SW	75S	
96	352	58NE	60S	R DS
97	130	52SW	65SE	R DS
98	160	22SW	175	
99	160	52SW	34S	
100	154	43SW	50S	
101	170	67SW	37S	
102	184	82W	27S	SS
103	190	55W	22S	SS
104	177	70W	24S	
105	170	67W	25S	
106	170	73SW	25S	
107	163	80SW	47S	
108	175	84SW	20S	
109	160	44SW	35S	
110	174	80SW	27S	
111	150	57SW	58S	
112	140	54SW	62S	
113	138	75SW	65S	
114	146	56SW	60S	
115	134	44W	60S	
116	110	35S	85SE	
117	147	65SW	45SE	
118	138	82SW	75SE	
119	103	33SW	78SE	
120	150	53SW	45SE	
121	125	77SW	52SE	
122	357	78NE	30S	
123	148	75SW	47S	
124	168	74SW	32S	
125	146	86SW	38S	

Table B. cont'd

Site number	Strike	Dip	Rake	Sense
126	176	62SW	30SW	
127	170	62SW	45S	
128	168	84SW	35S	
129	160	75SW	28S	
130	156	56SW	53S	
131	163	56SW	25S	
132	160	64SW	46S	
133	159	74SW	48S	
134	348	85NE	42S	N
135	24	68SE	52S	R DS
136	152	73SW	45S	
137	160	82SW	45S	
138	155	54SW	58S	
139	160	75SW	44S	
140	148	67SW	45S	
141	163	82SW	30S	R DS
142	156	80SW	48S	
143	148	45SW	54S	R
144	155	47SW	52S	R
145	3	76SW	75S	
146	156	64SW	60S	
147	168	67SW	45S	
148	164	80SW	50S	
149	180	75W	73S	
150	159	67SW	90	
151	157	50SW	82S	
152	342	89NE	90	
153	62	30S		
154	156	60SW	68S	
155	145	66SW	82S	
156	345	75NE	80S	
157	152	60SW	85S	
158	82	82SW	30S	

Table B. cont'd

Site number	Strike	Dip	Rake	Sense
159	90	45S	89S	
160	210	40N	40N	N DS